Universidade de Aveiro

2015

Secção Autónoma de Ciências da Saúde

Christian André Fernandes Neves

A glicação induzida por metilglioxal causa alterações do conteúdo lipídico-hepático e dismetabolismo em ratos com dieta gorda

Methylglyoxal-induced glycation changes liver lipid content in high-fat diet-fed rats, causing glucose and lipid systemic dysmetabolism

Tese apresentada à Universidade de Aveiro para cumprimento dos requisitos necessários à obtenção do grau de Mestre em Biomedicina Molecular, realizada sob a orientação científica do Doutor Paulo Matafome, Professor Adjunto, Escola Superior de Tecnologia da Saúde de Coimbra e Investigador do Laboratório de Fisiologia do Instituto de Imagem Biomédica e Ciências da Vida da Faculdade de Medicina da Universidade de Coimbra. Co-orientação científica da Professora Doutora Odete Cruz e Silva, Professora Auxiliar com Agregação da Secção Autónoma de Ciências da Saúde da Universidade de Aveiro.

Este trabalho teve o apoio do Laboratório de Fisiologia, Institute of Biomedical Imaging and Life Sciences e do Instituto de Ciências Nucleares Aplicadas à Saúde da Faculdade de Medicina da Universidade de Coimbra e do QOPNA do Departamento de Química da Universidade de Aveiro e foi financiado pelo projeto FCT (Pest-C/SAU/UI3282/2011), FEDER-PT2020 (002034 and 00205), FCT/MEC (UID/QUI/00062/2013), DoIT – Diamarker (QREN- COMPETE) and RNEM (REDE/1504/REM/2005).

Dedico este trabalho à família e amigos...

o júri

presidente

Doutora Ana Gabriela da Silva Cavaleiro Henriques
Professora Auxiliar Convidada, Universidade de Aveiro

Professora Doutora Maria do Rosário Gonçalves dos Reis Marques Domingues
Professora Auxiliar com Agregação, Universidade de Aveiro

Doutor Paulo Nuno Centeio Matafome
Professor Adjunto, Escola Superior de Tecnologia da Saúde de Coimbra

agradecimentos

Ao concluir mais uma etapa da minha caminhada académica, quero agradecer a todos os que, com o seu conhecimento, disponibilidade, partilha, motivação e entusiasmo, foram fundamentais para ultrapassar as dificuldades e sempre estiveram ao meu lado.

Desta forma, deixo apenas algumas palavras, poucas, mas com um sentido e profundo sentimento de reconhecido agradecimento.

À *Professora Doutora Raquel Seiça*, por me proporcionar as condições necessárias para estagiar e elaborar a minha tese, por permitir a minha integração num centro de investigação e pela simpatia e disponibilidade para me orientar neste percurso académico e científico.

Ao *Doutor Paulo Matafome,* quero expressar o meu profundo agradecimento pela orientação, apoio, aprendizagem técnica e cientifica e por me incentivar a continuar a fazer melhor. Obrigado também pela confiança e responsabilidade que me incutiu ao longo deste ano e meio e obrigado porque, mais do que um orientador e professor, se tornou um grande amigo que quero levar para a vida. O sentido de humor e profissionalismo são atitudes que bem aplicados tornam as pessoas as melhores que alguém poderia conhecer. Obrigado também por permitir a minha presença nos congressos com o projeto, pelos prémios e submissão de publicações futuras.

À Coordenadora do mestrado, *Professora Doutora Odete Cruz e Silva*, pela orientação, oportunidade e privilégio por permitir a minha frequência no mestrado em Biomedicina Molecular, apesar de todos os contratempos. Um especial agradecimento também às coordenadoras da licenciatura e mestrado *Doutora Margarida Fardilha* e *Doutora Ana Gabriela Henriques* pelo apreço e motivação.

À *Professora Doutora Rosário Domingues*, que tive o privilégio de conhecer na minha licenciatura e que desde esse momento se tornou uma professora muito especial pela simpatia e dedicação. Obrigado por possibilitar a realização deste projeto no seu laboratório, pela confiança e por toda a colaboração, que contribuiu fundamentalmente para a minha formação.

Aos meus colegas do Laboratório de Fisiologia pela amizade, companheirismo, pela ajuda, aprendizagem e aventuras. Em especial para o Doutorando Tiago Rodrigues, Rita Fonseca, Luís Gamas, José Paulo e às aquisições recentes e transitórias Guida, Amina, Elinor, Judith e Roselyne.

Ao *Professor Doutor Miguel Castelo Branco, ao Doutor José Sereno* e restante equipa do ICNAS, com quem tive o privilégio de colaborar e que mantêm o incentivo na continuação do trabalho.

À *Doutora Cláudia Simões*, que me ajudou criteriosamente na lipidómica. Obrigado pela sua exigência e total disponibilidade. Obrigado também à Técnica Superior D. Cristina Barros pela entreajuda, carinho e bom sentido de humor diário que tornou os meus dias mais alegres durante a colaboração no QOPNA, pelo companheirismo e boa disposição. Obrigado também à restante equipa pelos momentos bem passados.

Ao Sr. Simões da Fisiologia pela alegria e apoio prestado.

Ao Serviço de Patologia Clínica do Centro Hospitalar Universitário de Coimbra pela colaboração nas análises sistémicas.

À Técnica Ana Marau pela manutenção do Biotério do IBILI.

Aos meus professores do colégio Fátima, da ESE e da Universidade de Aveiro que sempre contribuíram para fazer de mim um homem melhor, enriquecendo a minha vida e formação académica e científica. Em especial à *Doutora Ilka Martins*, à *Doutora Vera Afreixo,* ao *Doutor José Mesquita Bastos*, ao *Professor Doutor António Amaro* e ao Professor *Doutor Pedro Domingues* pelo exemplo e motivação.

À família, aos meus pais pelo seu apoio incondicional, padrinhos, irmãos, sobrinhos, tios e primos.

Um agradecimento especial à minha mãe pela “estudante” exemplar que tem sido, sempre disponível para me ajudar, bem como à minha irmã que, por telefone ou mail, tem partilhado os seus conhecimentos e experiência médica, esclarecendo dúvidas e tornando a Venezuela mais perto de Portugal e ainda à minha prima Isabel, pelo grande carinho e pelas tardes e noites perdidas, ajudando-me a finalizar todo o trabalho.

Às minhas colegas de longa data académica, Inês Pinheiro e Lorrane pelo carinho, paciência, apoio e ajuda ao longo deste percurso que ainda se irá prolongar por largos anos. Obrigado por tudo... do fundo do coração.

À Romina que, apesar de longe nestes últimos anos, manteve sempre o contacto e apoio. Obrigado por todo o afeto e interminável amizade.

À Joana Simões, Mafalda e Raquel Lima pela parceria nos trabalhos “a sério”, amizade e por aturarem o meu “stress” do hepatócito.

À Catarina Toscano que, apesar de nos conhecermos há pouco tempo, já tem um lugar cativo. Obrigado pela paciência e bons momentos passados.

Às melhores pessoas da FMUC: João, Sílvia, Marta, Olga, Inês Figueiredo e Isabel, obrigado por me aturarem, por terem de ouvir as minhas desculpas da tese e pela pseudo-ausência na mesa quando me punha a escrever.

À minha fantástica turma 9/2 que me acolheu quando entrei em medicina, que me ajudou nos momentos mais difíceis e pela continuação como colegas médicos no futuro.

Aos meus amigos e companheiros sobreviventes do mestrado, pela força, incentivo e bons momentos. Obrigado especial à Filgas, Dani, Marta, Cátia e Margarida.

Aos meus amigos de CBM, em especial aos meus moleculares e farmacêuticos de 2009/2010, e a todos os que me acompanharam até 2013, principalmente à Coelha. Aos meus pedaços de terra e pseudo-afilhados pelo conforto, ajuda nos momentos mais precisos e pela compreensão, em especial à Diana, Mário e Pedro.

Aos meus amigos do CEL que, apesar de recentes, já deixaram a sua marca, principalmente ao Hugo pela amizade e presença.

Às coletividades a que pertenço: Grupo de Samba Os Morenos, Escuteiros CNE 233-Estarreja, Grupo de Teatro Artê, Associação Antigos Alunos Estarreja e Universidade Senior Rotary Estarreja, pela compreensão nas minhas ausências, por me aceitarem de papéis na mão para estudar ao mesmo tempo durante as atividades e pelo carinho demonstrado.

Aos amigos da ESE pelo apoio na integração numa nova realidade estudantil e pela amizade que perdura, em especial à Cíntia.

E, por último, mas não menos importante, aos meus “Miguitos” que sei que estarão sempre presentes quando preciso, que nunca me deixarão só e sempre me apoiarão. Um obrigado especial à Rosa, Marisa, Ju, Inês, Tiago, Dayana, Cátia, Bruno, Ricardo, César, Juan, Hugo, Rita Sá, Couras, Pedrinho, Tiaguinho, Joãozinho e Joaninha.

E obrigado a todos os outros que, mesmo não identificados, foram importantes com o seu incentivo e apoio permanentes, bem como a todas as pessoas amigas ou conhecidas, que têm manifestado o seu carinho e orgulho com o sucesso alcançado em cada momento da minha vida.

palavras-chave

Fígado gordo, lipotoxicidade, obesidade, insulino-resistência, diabetes mellitus tipo 2, metilglioxal, glicação

resumo

O fígado gordo é simultaneamente uma causa e consequência da diabetes mellitus tipo 2. O metabolismo lipidico-hepático (MLH) encontra-se alterado em obesos, causando insulino-resistência. A diminuição da sinalização da via da insulina pode igualmente afetar o MLH, estimulando o desenvolvimento de esteatose hepática, comum nos doentes. Neste trabalho, pretende-se analisar o papel da glicação (induzida por metilglioxal) no MLH em ratos com dieta gorda, através de técnicas de lipidómica e ressonância magnética, para identificar as espécies lipídicas hepáticas, tais como fosfolípidos (FL), triglicéridos (TG), diacilgliceróis (DAG) e ácidos gordos (AG). O modelo animal usado foi o rato Wistar, mantido nos últimos 4 meses, antes de completar 1 ano de idade, com metilglioxal (100mg/Kg/dia) (grupo MG), com dieta gorda rica em TG (grupo HFD) ou com ambas (grupo HFDMG) e comparados com os controlos com dieta normal (n=12/grupo). As técnicas de lipidómica usadas foram cromatografia líquida com espetrometria de massa e cromatografia gasosa para determinar a composição hepática de PL, TG e AG. Usou-se também espectroscopia (9 Tesla), não invasiva, de ressonância magnética nuclear ^{1}H (NMR) nos ratos vivos para determinar os TG e DAG hepáticos. Os mediadores proteicos totais e fosforilados da via da insulina e da oxidação lipídica no fígado também foram analisados por *western blot*. Os ratos, com dieta gorda (HFD), aumentaram o peso corporal, mas o efeito foi parcialmente inibido pelo metilglioxal (HFDMG). Além disso, o grupo HFDMG apresenta um aumento dos ácidos gordos livres no plasma, hiperinsulinemia, insulino-resistência e intolerância à glicose. No fígado, as técnicas de lipidómica e NMR mostraram um aumento da massa gorda no fígado nos grupos HFD e HFDMG, mas apenas no grupo HFD se verifica o aumento do AG 18:1 (comum na dieta). Apesar de não haver diferença significativa no grupo HFD, o grupo HFDMG apresenta uma diminuição dos AG insaturados e aumento dos saturados; isto deve-se à diminuição dos monoinsaturados neste grupo. Quanto à esterificação dos glicerolípidos, o grupo HFDMG apresenta uma menor percentagem da total esterificação dos gliceróis, sugerindo o aumento dos DAG, em relação aos TG. Também, este grupo apresenta um ratio AG/glicerol aumentado, ou seja, com aumento de AG não esterificados. A análise por *western blot* mostrou uma diminuição da via do receptor da insulina especialmente no grupo HFDMG. Em suma, estes resultados sugerem que a glicação causa alterações do metabolismo lipidico-hepático num contexto de hiperlipidemia, contribuindo possivelmente para a lipotoxicidade hepática, progressão acelerada de insulino-resistência e patologia do fígado gordo.

Keywords Fatty liver disease, lipotoxicity, obesity, insulin resistance, type 2 of diabetes mellitus, methylglyoxal, glycation

Abstract

Fatty liver disease is simultaneously a cause and a consequence of type 2 diabetes. Hepatic lipid metabolism is altered in obese patients, causing insulin resistance. More, inhibition of insulin signaling may also affect hepatic lipid metabolism, causing a feedback that may lead to hepatic steatosis, common in such patients. In this work, we intended to assess the role of glycation (methylglyoxal-induced) in the hepatic lipid metabolism of high-fat diet-fed rats, using lipidomic approaches and magnetic resonance imaging, which identify hepatic lipid species, including phospholipids (PL), triglycerids (TG), diacylglycerols (DAG) and fatty acids (FA). Wistar rats were maintained during 4 months with methylglyoxal (MG) supplementation (100mg/Kg/day) (MG group), a high-fat diet rich in TG (HFD group) or both (HFDMG group) and compared with controls feeding a standard diet (n=6/ group). Lipidomic approaches, namely liquid chromatography - mass spectrometry (LC-MS) and gas chromatography (GC) were used to determine liver composition in PL, TG and FA. Non-invasive ^{1}H nuclear magnetic resonance (NMR) spectroscopy (9 Tesla) of liver tissues in vivo was used to determine lipid species, such as TG and DAG. The total and phosphorylated levels of the mediators of the insulin receptor pathway and lipid oxidation were determined by western blotting. High-fat diet-fed (HFD) rats showed increased body weight in relation to controls, but this effect was partially inhibited by MG supplementation (HFDMG group). Moreover, HFDMG group showed increased plasma free fatty acid levels, hyperinsulinemia, insulin resistance and glucose intolerance. In liver, lipidomic techniques and ^{1}H NMR showed increased fat mass in the liver of HFD and HFDMG rats. HFD rats, but not HFDMG, showed increased total levels of the 18:1 fatty acid (common in high-fat diets). Despite no differences were observed for HFD group, HFDMG rats showed decreased fraction of unsaturated lipids and increased fraction of saturated lipids. This difference was obtained due to a decrease in monounsaturated FA. Regarding lipid esterification, HFDMG group showed lower percentage of esterified glycerol carbons, suggesting an increased concentration of DAG in relation to TG. In accordance, this group showed higher fatty acids/glycerol ratio, suggesting increased liver non-esterified fatty acid levels. Western Blotting analyses showed decreased activation of insulin pathway, especially HFDMG group, as well as decreased activation of the insulin receptor in HFDMG group. Data suggest that glycation changes lipid metabolism in a context of hyperlipidemia, possibly contributing to hepatic lipotoxicity and to accelerate progression of insulin resistance and fatty liver disease.

Poster Presentations at Scientific Meetings

Neves C, Sereno J, Simões C, Castelhano J, Gonçalves S, Fonseca R, Rodrigues T, Domingues R, Matafome P, Castelo-Branco M, Seiça R. Characterization of hepatic lipid content in rats with diet-induced glycation and obesity by lipidomic approaches and magnetic resonance spectroscopy. VI Annual Meeting of IBILI, Coimbra, Portugal, December 11-12, 2014.

Neves C, Sereno J, Simões C, Castelhano J, Gonçalves S, Fonseca R, Rodrigues T, Domingues R, Matafome P, Castelo-Branco M, Seiça R. Hepatic Lipid Profile in rats with diet-induced glycation and obesity. IV In4Med, Coimbra, Portugal, February 20-22, 2015 – Top 5 finalists of "I Concurso Fundação AstraZeneca".

T. Rodrigues, J.P. Almeida, J. Sereno, J. Castelhano, **C. Neves**, R. Fonseca, S. Gonçalves, L. Gamas, M. Castelo-Branco, P. Matafome, R. Seiça. Methylglyoxal impairs high-fat diet-induced adipose tissue expansion causing systemic dysmetabolism. 51st Annual Meeting EASD, Stockholm, Sweden, September 14-18, 2015.

P. Matafome, J. Sereno, J. Castelhano, T. Rodrigues, S. Gonçalves, **C. Neves**, C. Marques, R. Seiça, M. Castelo-Branco. Glycation and high-fat diet trigger distinct functional consequences in the heart: an MRI study. 51st Annual Meeting EASD, Stockholm, Sweden, September 14-18, 2015.

Scientific Distinctions/Awards

"Investigation Award" – Gala Solidária Asclepius. Núcleo de Estudantes de Medicina da Associação Académica de Coimbra, Coimbra, Portugal, February 18, 2015.

Manuscript Submissions

T. Rodrigues, J. Almeida, L. Gamas, J. Sereno, J. Castelhano, **C. Neves**, S. Gonçalves, A. Arslanagic, E. Wilcken, R. Fonseca, I. Simões, M. Castelo-Branco, P. Matafome, R. Seiça. "AGEing fat: methylglyoxal-induced glycation impairs adipose tissue expansion causing systemic dysmetabolism in high-fat diet-fed rats" – Diabetes Journal. July, 2015.

Index

List of tables

List of figures

Abbreviations

ACBP	Acyl-CoA Binding Protein
ACC	Acetyl-CoA Carboxylase
ACS	Acyl-CoA Synthetase
AdipoR	Adiponectin Receptor
AGE	Advanced Glycated End-products
Akt	Protein Kinase B
ALT	Alanine Aminotransferase
AMP	Adenosine Monophosphate
AMPK	AMP-activated Protein Kinase
AST	Aspartate Aminotransferase
ATP	Adenosine Triphosphate
Ca^{2+}	Calcium Ions
cAMP	Cyclic Adenosine Monophosphate
CBP	CREB Binding Protein
cHMG-CoA	Cytosolic Hydroxymethylglutaryl-Coenzyme A
ChREBP	Carbohydrate-Responsive Element Binding Protein
CL	Cardiolipin
CoA	Coenzyme A
CPT-I	Carnitine Palmitoyltransferase I (or also known as CPT1)
CPT-II	Carnitine Palmitoyltransferase II
CRE	cAMP Response Element
CREB	Cyclic-AMP Response Element-binding Protein
Ct	Control
DAG	Diacylglycerol
FA-CoA	Fatty Acid Coenzyme A
FABP	Fatty Acid Binding Protein
FAS	Fatty Acid Synthase
FAT	Fatty Acid Translocase
FATP	Fatty Acid Transport Protein
FBPase-2	Fructose-2,6-biphosphatase 2
FFA	Free Fatty Acid
G6Pase	Glucose-6-Phosphatase

GC-FID	Gas Chromatography – Flame Ionization Detector
GDP	Guanosine Diphosphate
GGT	Gamma Glutamyl Transferase
GK	Glucokinase (or also known as Hexokinase)
GLUT2	Glucose Transporter 2
GLUT7	Glucose Transporter 7
GPAT	Glycerophosphate Acyltransferase
GSK-3	Glycogen Synthase Kinase-3
GTP	Guanosine Triphosphate
HbA1c	Glycated Hemoglobin
HDL	High-density Lipoproteins
HFD	High Fat Diet
HFDMG	High Fat Diet and Methylglyoxal
HPLC-MS/MS	High Performance Liquid Chromatography – Tandem Mass Spectrometry
IDL	Intermediate-density Lipoproteins
IP_3R	Inositol-1,4,5-triphosphate Receptor
IR	Insulin Receptor
IRS-1	Insulin Receptor Substrate 1
JNK1	c-Jun N-terminal Kinase 1
LCAT	Lecithin-cholesterol Acyltransferase
LDL	Low-density Lipoproteins
LPC	Lysophosphatidylcholine
LPL	Lipoprotein Lipase
LXR	Liver X Receptor
LXRE	Liver X Receptor Element
MG	Methylglyoxal
mHMG-CoA	Mitochondrial Hydroxymethylglutaryl-Coenzyme A
MUFA	Monounsaturated Fatty Acid
NADPH	Nicotinamide Adenine Dinucleotide Phosphate
NAFLD	Non-alcoholic Fatty Liver Disease
NASH	Non-alcoholic Steatohepatitis
NEFA	Non-Esterified Fatty Acid
NF-κB	Nuclear Factor κB

NMR	Nuclear Magnetic Resonance
PA	Phosphatidic Acid
PC	Phosphatidylcholine
PDE3B	Phosphodiesterase 3B
PE	Phosphatidylethanolamine
PERK	Protein Kinase R-like Endoplasmic Reticulum Kinase
PFK-2	Phosphofructokinase 2
PG	Phosphatidylglycerol
PGC1-α	Peroxisome-proliferator-activated Receptor γ Coactivator 1 alpha
Pi	Inorganic Phosphate Group
PI	Phosphatidylinositol
PI3K	Phosphoinositide 3-kinase
PIP_2	Phosphatidylinositol 4,5-bisphosphate
PIP_3	Phosphatidylinositol 3,4,5-triphosphate
PKA	Protein Kinase A
PKB	Protein Kinase B (or also known as Akt)
PKC	Protein Kinase C
PL	Phospholipids
PPAR-α	Peroxisome Proliferator-activated Receptor alpha
PPRE	PPAR Response Element
PS	Phosphatidylserine
PUFA	Polyunsaturated Fatty Acids
ROS	Reactive Oxygen Species
RXR	Retinoid X Receptor
SCD1	Stearoyl-CoA Desaturase 1
SFA	Saturated Fatty Acids
SIK2	Salt-inducible Kinase 2
SM	Sphingomyelin
SREBP-1	Sterol Regulatory Element Binding Protein 1
SRE	Sterol Regulatory Element
TCA	Tricarboxylic Acid
TG	Triglycerides
TGF	Tumor Growth Factor

TLC	Thin Layer Chromatography
TLR4	Toll-like Receptor 4
TNF	Tumor Necrosis Factor
TORC2	Transducer of Regulated C 2
VLDL	Very-low-density Lipoproteins

CHAPTER 1

INTRODUCTION

Introduction

1. General Aspects

Liver and functions

The liver is one of the most metabolically active organs in the human body due to its functional capabilities, receiving 28% of the total blood flow and spending 20% of the oxygen used by the body. It is located in the middle of the peripheral blood circulation among the organs of the gastrointestinal system and the rest of the body, serving as a filter for portal blood with substances absorbed from the stomach, intestines and colon and released from the pancreas and spleen (see Figure 1).

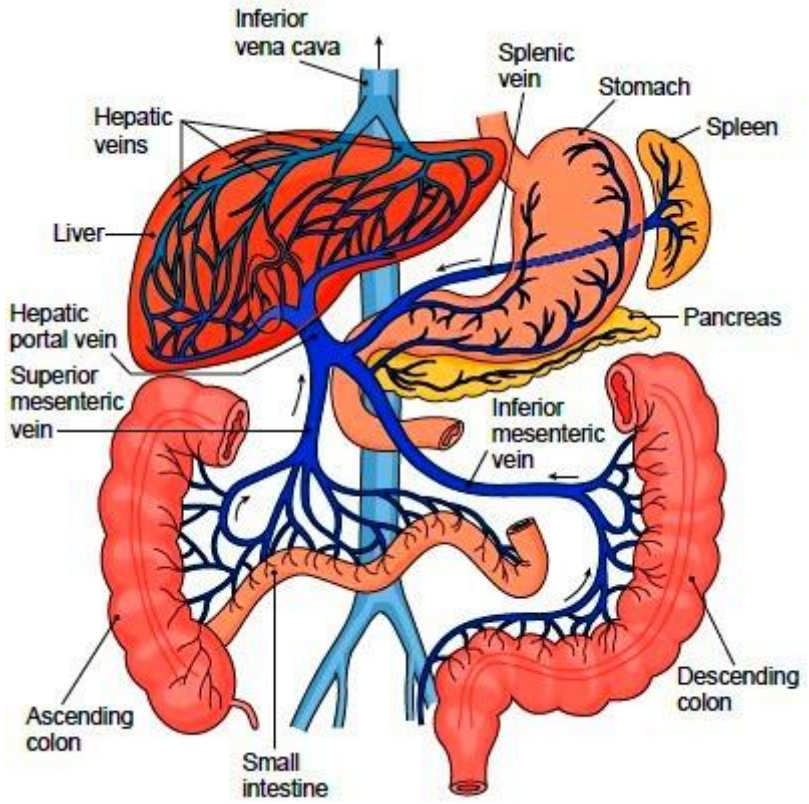

Figure 1: Hepatic Portal System. Arrows show the direction of blood flow(1).

Hepatocyte is the liver functional unity, organized in cordons of hexagonal lobules with a triad in each corner, composed of branches of the hepatic artery, portal vein and bile duct; the vessels drain to the center of the lobule where the central vein is(2). Periportal zone is more oxygenated, consequently this is specialized for oxidative metabolism like gluconeogenesis, amino acid catabolism, glycogenolysis, β–oxidation of fatty acids, cholesterol synthesis and degradation,

ureagenesis, bile synthesis and metabolic detoxification. Inversely, pericentral zone with lowest oxygen is responsible for biotransformations like glycolysis, glycogenesis (glycogen synthesis), liponeogenesis, ketogenesis, glutamine synthesis and drugs and xenobiotics activation or detoxification. Innervation, blood flow, concentration of substrates, oxygen and hormones influence the differential gene expression for different functions of catabolism or anabolism(3).

Thus, liver has a key role to metabolize, detoxify and produce compounds, serving as a biochemical factory, endocrine and exocrine gland and excretory system. It is capable to modify drugs, toxins or other compounds (activation or inactivation), to convert hormones and vitamins, to solubilize or conjugate substances and metabolites for excretion in the bile or urine. Liver can also synthesize carbohydrates, proteins and intermediate metabolites, and store carbohydrates, lipids, vitamins and minerals. Bile solute secretion is another important function of the liver to eliminate exogenous and endogenous products (cholesterol and bilirubin) and to digest and absorb lipids from the intestine(2).

Finally, the reticuloendothelial system from liver is 80% to 90% constituted for macrophages, named Kupffer Cells that help to remove foreign particles like bacteria, toxins, parasites and old red blood cells(2) and they may have some role in developing metabolic pathologies(4).

2. Glucose Metabolism

Glucose Absorption

Glucose is the principal substrate for energy metabolism and meals contain several macromolecules of carbohydrates (polysaccharides), which need to be digested and absorbed. Salivary and pancreatic α-amilase, when activated in the intestinal lumen, start the hydrolysis of polysaccharides; then, disaccharidase forms dissacharides in the membrane of the epithelium of duodenum and jejune and lastly maltase, sucrase and lactase transform dissacharides into molecules of glucose (80%), fructose (15%) and galactose (5%). Monossacharides absorption occurs mostly in duodenum and proximal jejune by active transport and consequently they are released to the portal blood(5).

Liver Glucose Homeostasis

The regulatory mechanism of glucose is mediated by negative feedback. Pancreas releases insulin, a hypoglycemic hormone, when glucose levels are elevated in the blood, but when the body is in hypoglycemia, pancreas releases a hyperglycemic hormone, glucagon. Consequently, liver responds to these hormones to maintain homeostasis of glucose levels, stimulating hepatocytes to

make gluconeogenesis and glycogenolysis to deliver glucose to the plasma by glucagon induction and stimulating glycogenesis and glycolysis to eliminate glucose from plasma by insulin signal.

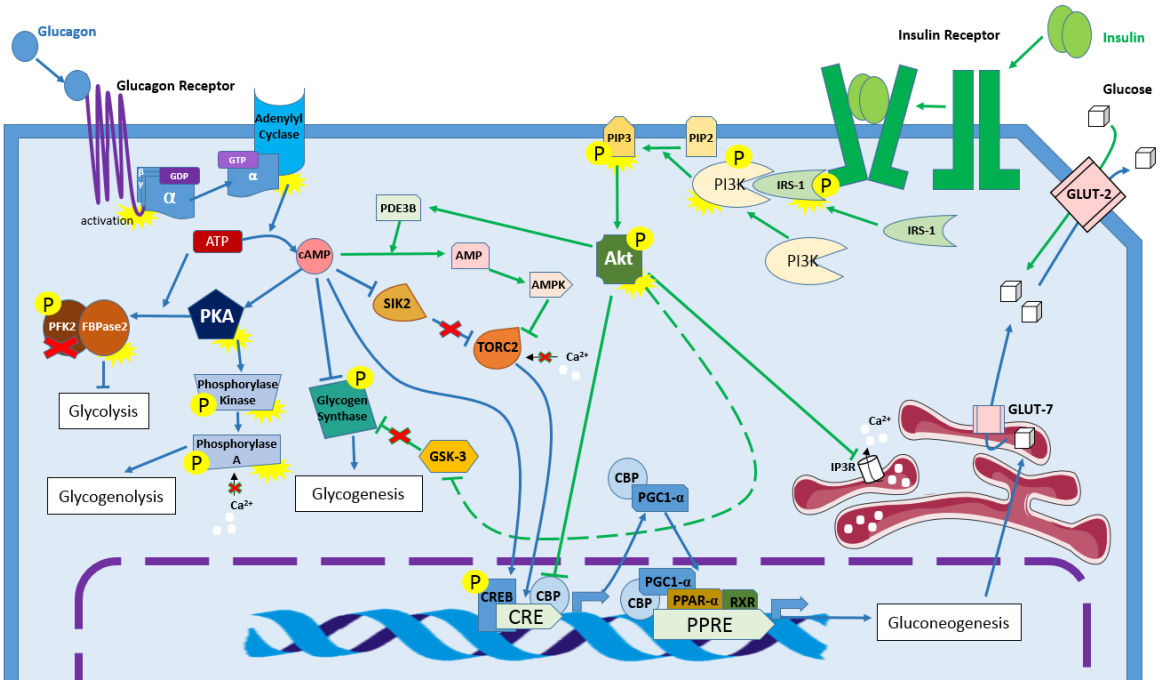

Figure 2: Liver Glucose Regulation by glucagon and insulin hormones. Blue pathway is influenced by glucagon and green pathway by insulin. Original Artwork). (GDP: Guanosine Diphosphate. GTP: Guanosine Triphosphate. ATP: Adenosine Triphosphate. cAMP: Cyclic Adenosine Monophosphate. PKA: Protein Kinase A. PFK2: Phosphofructokinase 2. FBPase2: Fructose-2,6-biphosphatase 2. P: Inorganic Phosphate Group (same as Pi). Ca2+: calcium ions. SIK2: Salt-inducible Kinase 2. TORC2: Transducer of Regulated C2. CREB: Cyclic-AMP Response Element-binding Protein. CRE: cAMP Response Element. CBP: CREB Binding Protein. PGC1-α: Peroxisome-proliferator-activated Receptor γ Coactivator 1. PPAR- α: Peroxisome Proliferator-activated Receptor alpha. RXR: Retinoid X Receptor. PPRE: PPAR Response Element. IRS-1: Insulin Receptor Substrate 1. PI3K: Phosphoinositide 3-kinase. PIP_2: Phosphatidylinositol 4,5-bisphosphate. PIP_3: Phosphatidylinositol 3,4,5-triphosphate. Akt: Protein Kinase B. PDE3B: Phosphodiesterase 3B. AMP: Adenosine Monophosphate. AMPK: AMP-activated Protein Kinase. IP_3R: Inositol-1,4,5-triphosphate Receptor. GSK-3: Glycogen Synthase Kinase-3. GLUT2: Glucose Transporter 2. GLUT7: Glucose Transporter 7.)

Glucagon Regulation

Gluconeogenesis is the process of *de novo* synthesis of glucose from amino acids and lactate in the endoplasmic reticulum, where exits by *Glucose Transporter 7* (GLUT7) to the cytoplasm and it is released into the bloodstream by *Glucose Transporter 2* (GLUT2)(2). Glycogenolysis is the cytosolic enzymatic process to breakdown glycogen stored into molecules of glucose.

Glucagon binds to *Glucagon Receptor* (G protein-coupled membrane receptor) in the hepatocyte, activating *Adenylyl Cyclase* to synthesize *Cyclic Adenosine Monophosphate* (cAMP), from *Adenosine Triphosphate* (ATP)(6). cAMP activates *Protein Kinase A* (PKA) to phosphorylate *Phosphorylase Kinase (active form)* and then this enzyme inactivate *Phosphorylase A*, promoting

the degradation of glycogen. Furthermore, cAMP interacts in a transcriptional phosphorylation cascade that ultimately activates in *Cyclic-AMP Response Element-binding Protein* (CREB) in the nucleus and it activates too the *Transducer of Regulated C*2 (TORC2) allowing its entrance in the nucleus, resulting in the activation of transcriptional factor *cAMP Response Element* (CRE) that leads to the expression of *Peroxisome-proliferator-activated Receptor γ Coactivator 1* (PGC1-α). PGC1-α binds to nuclear receptor *Peroxisome Proliferator-activated Receptor alpha* (PPAR-α) and forms a heterodimer with *Retinoid X Receptor* (RXR) in *PPAR Response Element* (PPRE) resulting in higher expression of enzymes necessary for Gluconeogenesis(7). cAMP also leads to phosphorylation and inactivation of the Glycogen Synthase through the Glycogen Synthase Kinase 3 (GSK3), thus inhibit glycogen synthesis. PKA phosphorylates a complex *Phosphofructokinase 2* (PFK-2), changing its conformational structure and exposing the active form of *Fructose-2,6-biphosphatase 2* (FBPase-2) to inhibit glycolysis(8).

Insulin Regulation

Glycogenesis is the process that forms glycogen from glucose to stores and Glycolysis is the process to spend glucose to transform it into energy.

To do this, it is necessary the dimerization of two molecules of insulin bounded in two insulin receptors (membrane tyrosine kinase receptor), to activate the signal cascade by autophosphorylation. Then, it is formed a local to bind the *Insulin Receptor Substrate 1* (IRS-1), phosphorylating it and activating the *Phosphoinositide 3-kinase* (PI3K); PI3K converts *Phosphatidylinositol 4,5-bisphosphate* (PIP_2) into *Phosphatidylinositol 3,4,5-triphosphate* (PIP_3) and then it is possible to phosphorylate and activate serine/threonine kinase *Protein Kinase B* (PKB, or also known as Akt). Akt phosphorylates *Phosphodiesterase 3B* (PDE3B), *Inositol-1,4,5-triphosphate Receptor* (IP_3R) in smooth endoplasmic reticulum, *CREB Binding Protein* (CBP) and *Glycogen Synthase Kinase-3* (GSK-3). PDE3B hydrolyses cAMP to AMP, reducing its hyperglycemic effects and *Adenosine Monophosphate* (AMP) activates *AMP-activated Protein Kinase* (AMPK) inhibiting TORC2. CBP is also inactivated by Akt, reducing transcriptional cascade of CRE, important for gluconeogenesis. GSK-3 phosphorylations and inactivation allows the activation of Glycogen Synthase increasing the formation of glycogen(7).

This regulatory mechanism is important because hypoglycemic levels could be mortal and chronic hyperglycemic levels lead to diabetes(7).

3. Lipid Metabolism

Lipid Absorption

Lipids are essential biomolecules to store energy in form of fatty acids or non-toxic form – triglycerides (TG). Thus, they are synthesized *de novo* or ingested and absorbed in the small intestine by enterocytes. Emulsified fat droplets contain phospholipids and bile salts with TG, cholesterol and vitamins and when arrive to small intestine, enterocytes break down TG into monoglycerides or fatty acids by pancreatic lipase. Then, these components are absorbed by diffusion; monoglycerides and fatty acids are re-esterified into triglycerides and along with other fats are enclosed in smooth endoplasmic reticulum and coated with proteins to form chylomicrons. Chylomicrons are exocytosed to the lymphatic vessels, then pass into the blood to deliver fats to the peripheral tissues and organs, including adipose tissue; cholesterol-rich remnant chylomicrons reach to the liver, where they are recycled, *de novo* synthesized, re-esterified and transported to the blood again in *Very-low-density Lipoprotein* (VLDL), containing apoprotein B-100 and C-II, triglycerides and cholesterol (see Figure 3).

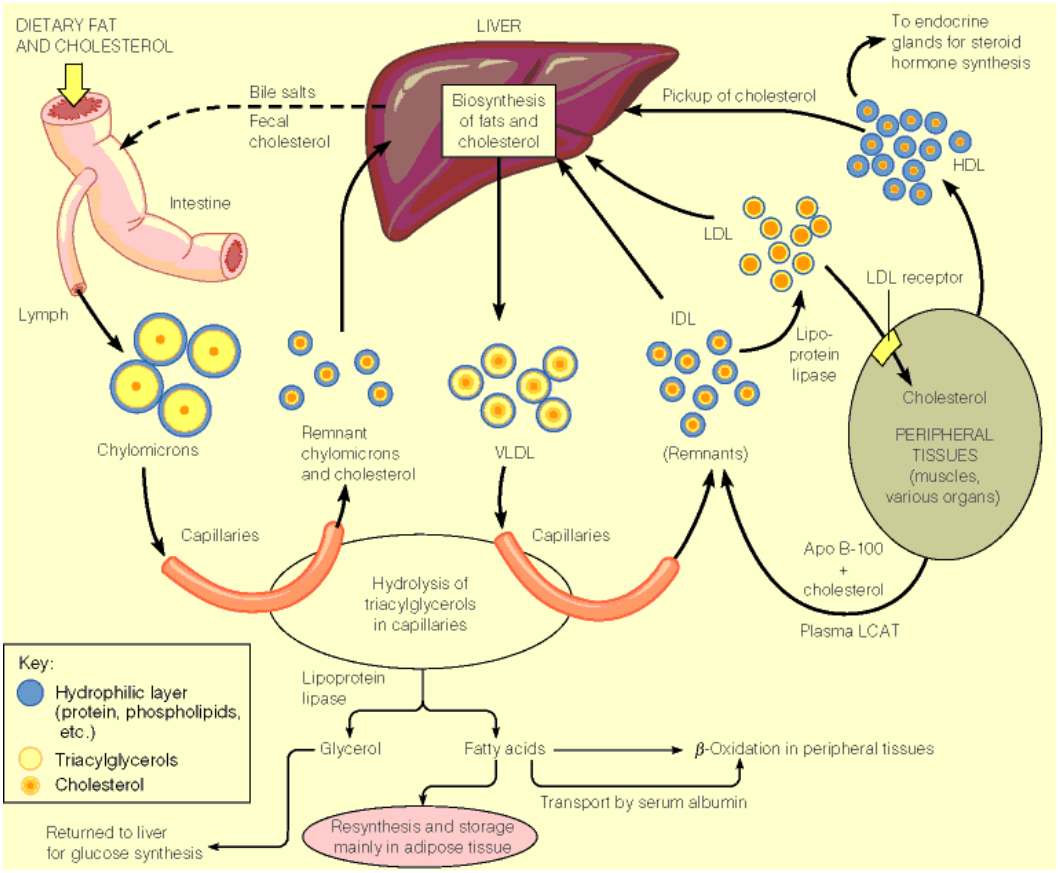

Figure 3: Lipid Metabolism(9). *(VLDL: Very-low-density Lipoproteins. IDL: Intermediate-density Lipoproteins. LDL: Low-density Lipoproteins. HDL: High-density Lipoproteins. LCAT: Lecithin-cholesterol Acyltransferase.)*

VLDL secretion is the mechanism that liver has to reduce Free Fatty Acids (FFA) and remnant lipoproteins, producing TG and cholesterol to be used by the cells or stored by adipose tissue. Apoprotein C-II activates endothelial *Lipoprotein Lipase* (LPL) to take fatty acids and glycerol from the VLDL, increasing cholesterol content. Liver and enterocytes can synthesize *High-density Lipoprotein* (HDL) with apoprotein A capable to take oxidized cholesterol (oxysterols) excess from peripheral tissues, redirect to the endocrine glands for steroid synthesis or go back to the liver for bile salts synthesis. Chylomicrons, VLDL, IDL and LDL are lipoproteins with type B and C apoproteins and HDL has type A and C apoproteins(2).

Liver can recycle absorbed fats or remnants of lipoproteins and it is capable to synthesize *de novo* – Lipogenesis. Fatty acids are synthesized *de novo* or founded in adipocytes-stored triglycerides, in the circulation in FFA form or in the lipoproteins in TG form(10).

Liver fatty acids uptake

Fatty acids are obtained through the hydrolysis of lipoproteins and chylomicrons by lipases and thioesterases, forming *Non-Esterified Fatty Acid* (NEFA) or *Fatty Acid Coenzyme A* (FA-CoA), respectively. Long-chain fatty acids (14 carbons or more) enter in hepatocytes from the blood in proportion to their concentration; they may be uptake as FFA, NEFA and FA-CoA by diffusion, *Fatty Acid Translocase* (FAT) and *Fatty Acid Transport Protein* (FATP), respectively (see Figure 4A).

FFA are plasmatic non-esterified fatty acids, released by adipocytes during lipolysis into to peripheral blood, bounded to albumin. Glucagon stimulates adipose tissue lipolysis releasing FFA, for use as a fuel by tissues and in liver, they are oxidized, serve as substrates for ketogenesis, inhibits glucose oxidation and stimulates gluconeogenesis (7,11).

NEFA is bound to *Fatty Acid Binding Protein* (FABP) and enter in the nucleus to regulate gene expression necessary for oxidation or synthesis of complex lipids (TG and phospholipids). *Acyl-CoA Synthetase* (ACS) is an outer-membrane mitochondrial enzyme that esterified NEFA to FA-CoA and then it is capable to bind to the *Acyl-CoA Binding Protein* (ACBP) which transport FA-CoA into the mitochondrion or deviate to peroxisomes (10).

The most frequent exogenous fatty acids are saturated and monounsaturated; they are palmitic acid (16:0 – 16 carbons and zero double bonds), stearic acid (18:0 – 18 carbons and zero double bonds) and oleic acid (18:1 – 18 carbons and one double bond). Linoleic acid (18:2) and linolenic acid (18:3) are essential unsaturated fatty acids, because mammals cannot introduce double bonds beyond 9^{th} position, so they become essentials in food due to metabolic pathways importance (12).

Lipogenesis

Liver lipogenesis is the process that transforms acetyl-CoA into fatty acids, which are used to produce energy by β-oxidation or to synthesize phospholipids and glycerolipids in hepatocytes. Fatty acids synthesized could be released in triglycerides-VLDL form or in ketone bodies to the peripheral tissues, by insulin or glucagon mediation, respectively. Acetyl-CoA is formed from glucose or acetate and its reaction start by addition of "primers units" of other acetyl-CoA; this reaction is catabolized by a decarboxylation enzymatic cascade with *Acetyl-CoA Carboxylase* (ACC) desphosphorilated (active form). ACC is phosphorylated and inhibited by elevated levels of FA-CoA and AMPK (see Figure 5), reducing malonyl-CoA levels and promoting β-oxidation of fatty acids(13).

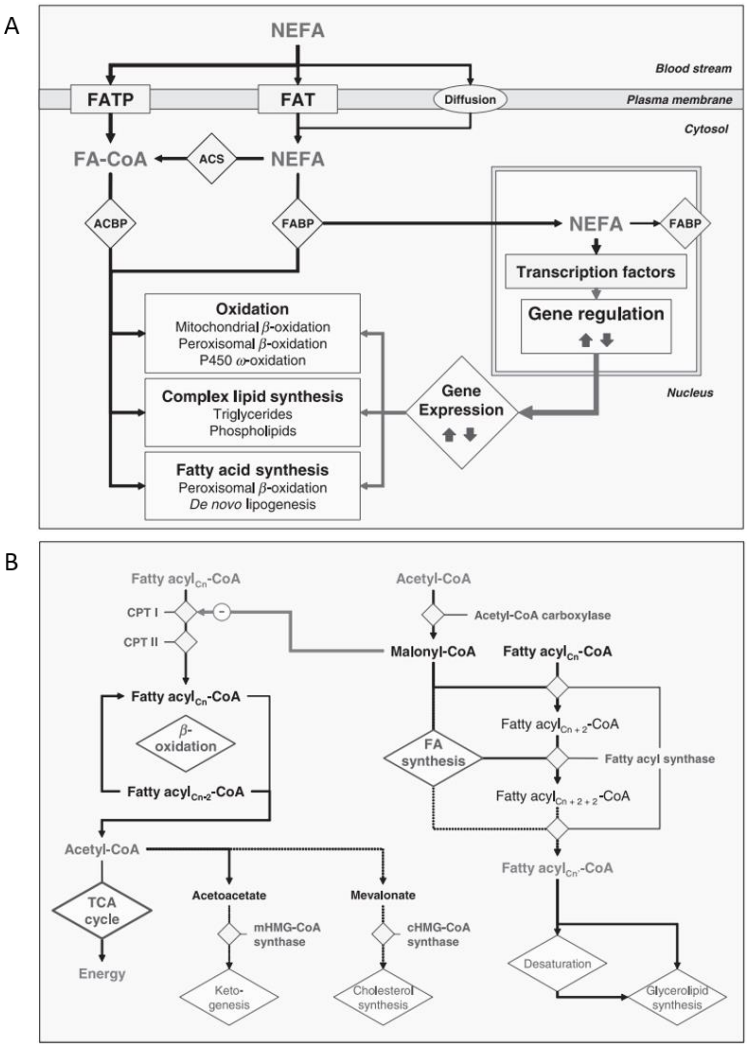

Figure 4: A: Liver fatty acids uptake, intracellular activation and functional pathways. B: Principal steps of synthesis and oxidation of fatty acids(10)*. (NEFA: Non-Esterified Fatty Acid. FAT: Fatty Acid Translocase. FATP: Fatty Acid Transport Protein. FA-CoA: Fatty Acid Coenzyme A. ACS: Acyl-CoA Synthetase. ACBP: Acyl-CoA Binding Protein. FABP: Fatty Acid Binding Protein. FA: fatty acid. Cn: chain of fatty acyl, Cn+2: malonyl-CoA unit addition. CPT-I: Carnitine Palmitoyltransferase I. CPT-II: Carnitine Palmitoyltransferase II. mHMG-CoA: Mitochondrial Hydroxymethylglutaryl-Coenzyme A. cHMG-CoA: Cytosolic Hydroxymethylglutaryl-Coenzyme A. TCA: Tricarboxylic Acid.)*

Extension reaction occurs using a second enzyme called *Fatty Acid Synthase* (FAS) and forms fatty acyl-CoA chain, which could react to synthesize fatty acids/glycerolipids or goes to mitochondrion for β-oxidation, regulated by glucagon and insulin, respectively (see Figure 4B).

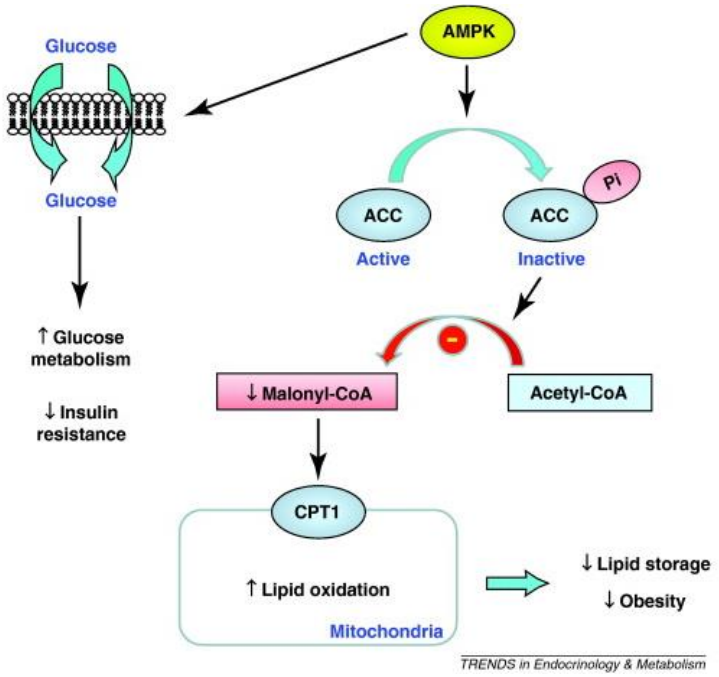

Figure 5: ACC inactivation by AMPK. ACC phosphorylated prevents malonyl-CoA formation, stimulating β-oxidation(14) *(AMPK: AMP-activated Protein Kinase. ACC: Acetyl-CoA Carboxylase. Pi: Inorganic Phosphate Group. CPT1: Carnitine Palmitoyltransferase I.)*

If synthesis happens, fatty acyl-CoA chain reacts with FAS until the formation of palmitic acid (16:0) by elongation process, requiring *Nicotinamide Adenine Dinucleotide Phosphate* (NADPH), and then this fatty acid can elongate and/or desaturate by different enzymes. Desaturases are endoplasmic reticulum oxidases that convert saturated or unsaturated fatty acids into polyunsaturated fatty acids. Stearoyl-CoA desaturase 1 (SCD1) is the principal desaturase which catalyzes the D^9-cis desaturation of palmitoleyl-CoA (16:0) and oleoyl-CoA (18:0), from *de novo* synthesis or diet (see Figure 6), reducing saturated fatty acids. Monounsaturated fatty acids (MUFA) are in turn used to synthesize glycerolipids or phospholipids. SCD1 expression increases with high-carbohydrate, high-saturated and high-monounsaturated diets, by the activation of *Sterol Regulatory Element Binding Protein* (SREBP-1) via insulin or oxysterols(15). SCD1 stimulates ACC and Akt and inhibits AMPK(16).

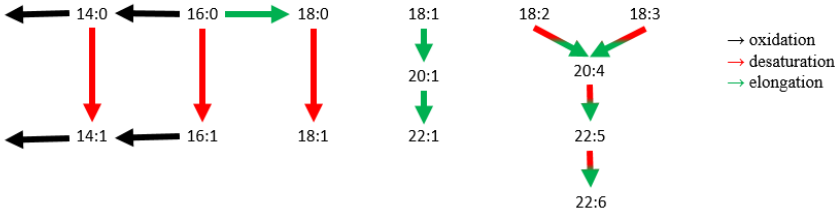

Figure 6: Reactions of oxidation, elongation and desaturation of principal exogenous fatty acids.

Lipogenesis gene expression is regulated by insulin and oxysterols that activate transcription factors, namely the SREBP-1 and nuclear receptor *Liver X Receptor* (LXR) (see Figure 7). Oxysterols are oxidized cholesterol from lipoprotein that bind to LXR, activate transcription factor *Liver X Receptor Element* (LXRE), which promotes gene expression of SREBP-1 and inhibition of cholesterol synthesis. SREBP-1 is activated by Akt, enter in the nucleus and stimulates *Sterol Regulatory Element* (SRE) for gene expression of essential enzymes for fatty acids synthesis (ACC and FAS) and glycolysis (*Glucokinase* – GK)(17,18).

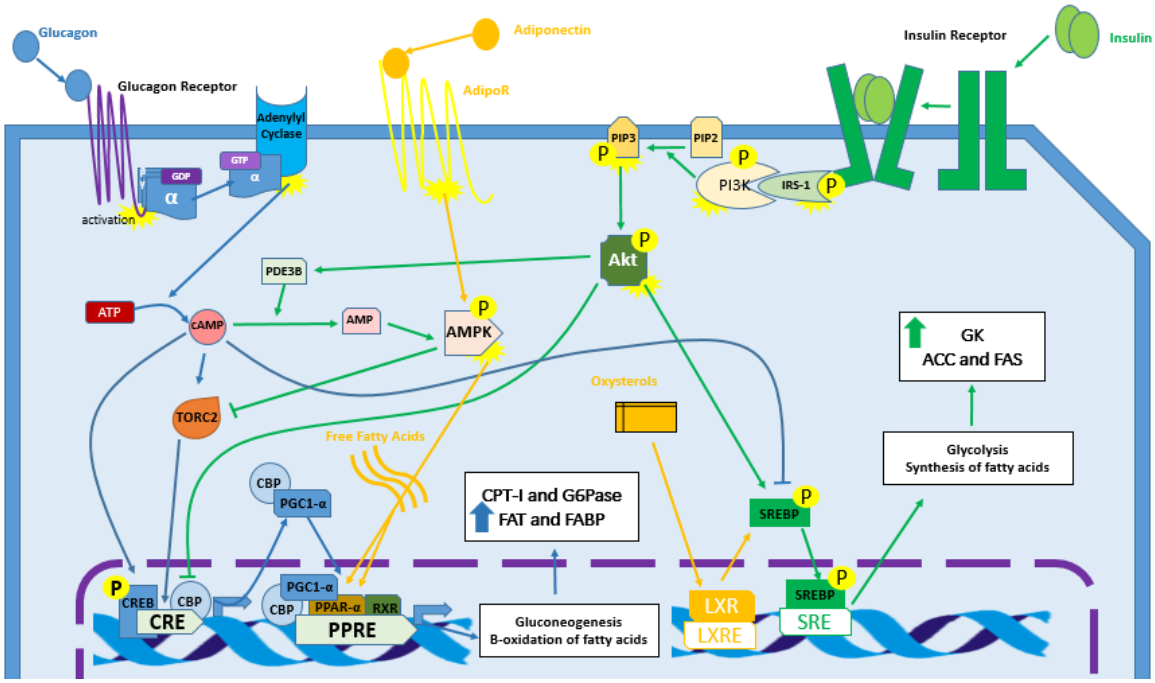

Figure 7: Liver lipid regulation pathways mediated by insulin and glucagon. Blue pathway is influenced by glucagon and green by insulin. Original Artwork. (GDP: Guanosine Diphosphate. GTP: Guanosine Triphosphate. ATP: Adenosine Triphosphate. cAMP: Cyclic Adenosine Monophosphate. P: Phosphate group. TORC2: Transducer of Regulated C. CREB: Cyclic-AMP Response Element-binding Protein. CRE: cAMP Response Element. CBP: CREB Binding Protein. PGC1-α: Peroxisome-proliferator-activated Receptor γ Coactivator 1. PPAR- α: Peroxisome Proliferator-activated Receptor alpha. RXR: Retinoid X Receptor. PPRE: PPAR Response Element. IRS-1: Insulin Receptor Substrate 1. PI3K: Phosphoinositide 3-kinase. PIP2: Phosphatidylinositol 4,5-bisphosphate. PIP3: Phosphatidylinositol 3,4,5-triphosphate. Akt: Protein Kinase B. PDE3B: Phosphodiesterase 3B. AMP: Adenosine Monophosphate. AMPK: AMP-activated Protein Kinase. LXR: Liver X Receptor. LXRE: Liver X Receptor Element. SREBP-1: Sterol Regulatory Element Binding Protein 1. SRE: Sterol Regulatory Element. GK: Glucokinase, or also known as Hexokinase. ACC: Acetyl-CoA Carboxylase. FAS: Fatty Acid Synthase. GPAT: Glycerophosphate Acyltransferase. CPT-I: Carnitine Palmitoyltransferase I. G6Pase: Glucose-6-Phosphatase. FAT: Fatty Acid Translocase. FABP: Fatty Acid Binding Protein. AdipoR: Adiponectin receptor).

Glycerolipid Synthesis and VLDL Exportation

Glycerol-3-phosphate from glycolysis is transferred to fatty acyl chain synthesized by *Glycerophosphate Acyltransferase* (GPAT); consecutively, *Lysophosphatidate Acyltransferase* and *Diacylglycerol Acyltransferase* lead to formation of *Diacylglycerol* (DAG) and TG (see Figure 15). This mechanism is activated when NEFA is elevated, when phospholipids in the membrane are overloaded or SREBP-1 are elevated, increasing ACC, FAS and GPAT (see Figure 7).

Insulin promotes glycogenesis by glycogen synthase and glycolysis and fatty acid synthesis by SREBP-1. This reduce glucose from plasma, form glycogen and ATP by glycolysis, increasing cellular fuel supplies and form triglycerides(10). AMPK levels are essential to understand regulation of lipid metabolism, because AMPK is decreased when fuel supplies are elevated, but when fuel supplies and ATP are reduced, like after exercise, AMPK is increased due to PDE3B activation that reduces cAMP in AMP, activating AMPK(19); when the needs are satisfied, AMPK turn down again. AMPK phosphorylates ACC, inhibiting fatty acid synthesis and stimulating β-oxidation by reduction of malonyl-CoA; more, AMPK inactivates GPAT and inhibits cholesterol and glycogen synthesis(see Figure 5)(10).

Synthesis of lipoproteins, namely VLDL, is important to export triglycerides and cholesterol to the bloodstream. There is only one apoprotein B100 per VLDL particle; it is synthesized in rough endoplasmic reticulum and assembled in the phospholipids, in smooth endoplasmic reticulum. Then, in the Golgi complex, apoprotein is glycosylated and it is released into blood in VLDL form. Carbohydrates-rich ingestion and FFA increase upregulate esterification and lipoprotein synthesis, without *de novo* synthesis(10). More than normal insulin levels inhibit lipoprotein synthesis, independently of FFA levels(3). TG are stored in Lipid droplets within the hepatocyte or processed to VLDL(20). FFA exacerbate hepatic esterification and VLDL production by the increase of expression of microsomal triacylglycerol transfer protein and stability of apoprotein B, such as occur with high-fat diets and when excess adipose tissue releases FFAs directly into the circulation (eg, in obesity, uncontrolled diabetes mellitus)(3,10). VLDL is the way the liver exports excess TGs derived from plasma FFA and chylomicron remnants; VLDL synthesis increases with increase in intrahepatic FFA. It is known that in rats, stored hepatic triglycerides in lipid droplets do not participate directly in VLDL production, only after lipolysis of lipid droplet by microsomal lipase, generating NEFA and DAG (and eventually monoacylglycerols). After that, DAG could be re-esterified in microsomal membrane by DAG acyltransferase and translocated into the lumen to incorporation in VLDL(10). TG synthesis is under control by SREBP-1, *Carbohydrate-Responsive Element Binding Protein* (ChREBP), PPARα, LXR and ligands(10).

Phospholipid Synthesis

Glycerophospholipids are constituted by two fatty acids, one glycerol, one phosphorous group and a head (choline, ethanolamine, serine, inositol or other glycerol), forming phosphatidylcholine (PC), phosphatidylethanolamine (PE), phosphatidylserine (PS), phosphatidylinositol (PI) and phosphatidylglycerol (PG). Cardiolipins (CL) are phospholipids with the combination of PG and cytidine-diphosphate-acylglycerol, with four fatty acids. Lysophosphatidylcholine (LPC) has only one fatty acid, while sphingomyelin (SM) is a PC head group and a ceramide (see Figure 8)(12).

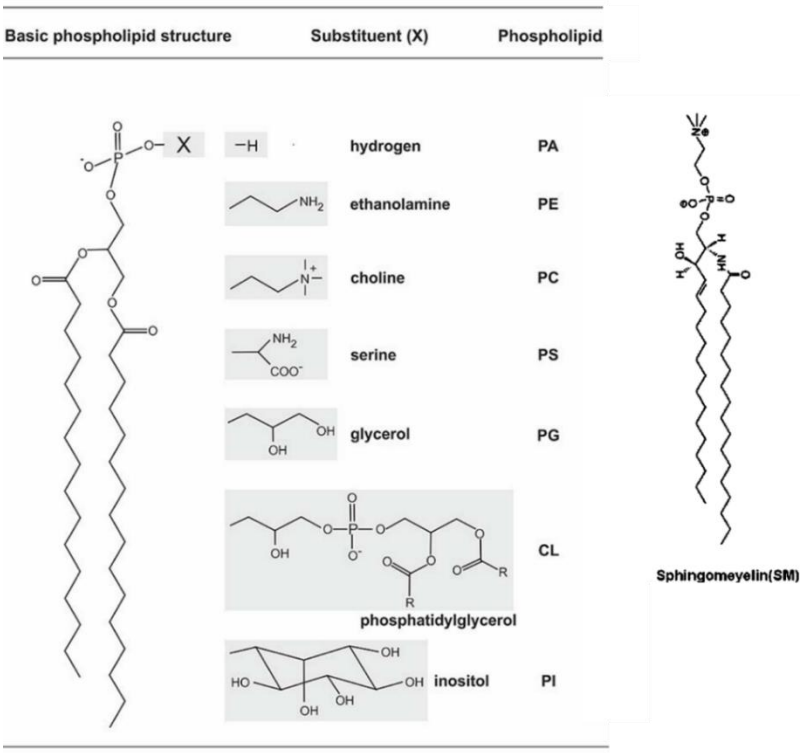

Figure 8: Chemical structure of phospholipids

Phospholipids (PL) are the principal component in cellular and organelle membranes; they have several functions, regulating the flexibility, selective permeability and fusion capacity of the cellular membrane and they interact in signal transduction and energetic process. PC are the major component in biological membranes, then followed by PE and PS. Minor PL components of biological membranes are SM, PG, PI and LPC - a class derived from PC, resulting from partial hydrolysis. CL are present in inner mitochondrial membrane. 1-10% of all PI are PIP_2, an important signal molecule in insulin pathway (see Figure 2)(12). PC and PE plasmalogens contain a hydrocarbon chain, linked to glycerol Carbon1 by a vinyl ether linkage and they are associated to antioxidant effects(21). PL synthesis starts in smooth endoplasmic reticulum, like TG, and is

transported to the Golgi complex to finish its assembling and finally they are transported to the membranes. This process also allows to reduce the levels of fatty acids(12).

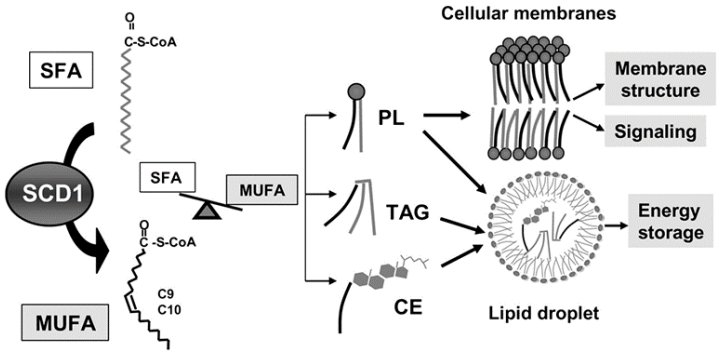

Figure 9: Monounsaturated fatty acids pathway(16) *(SFA: saturated fatty acid. SCD1: Stearoyl-CoA desaturase. MUFA: monounsaturated fatty acids. PL: phospholipids. TAG: triglycerides. CE: cholesterol esters.)*

Mitochondrial fatty acid oxidation

Non-esterified acyl-CoA are oxidized in different organelles depending on the chain length; mitochondrion oxidizes fatty acyl chains with more than 14 carbons and peroxisomes oxidizes very long chain fatty acids (>24 carbons). β-oxidation transforms fatty acid chain into acetyl-CoA units by *Carnitine Palmitoyltransferase I* (CPT-I) (outer membrane of mitochondrion) and *Carnitine Palmitoyltransferase II* (CPT-II) (inner mitochondrion membrane)(10) (see Figure 10). Gluconeogenesis and elevated levels of malonyl-CoA inhibit CPT-I (see Figure 4).

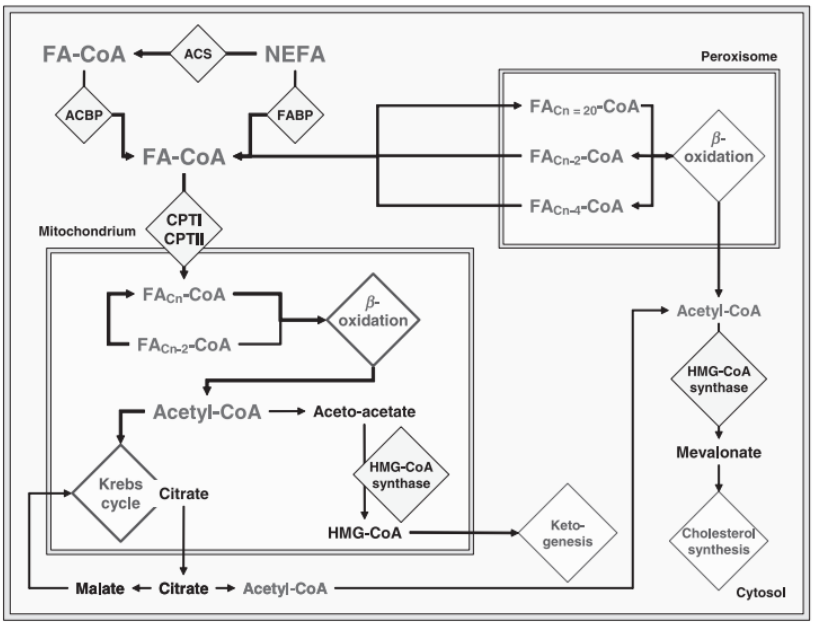

Figure 10: Fatty acid oxidation pathway (NEFA: Non-Esterified Fatty Acid. FAT: Fatty Acid Translocase. FATP: Fatty Acid Transport Protein. FA-CoA: Fatty Acid Coenzyme A. ACS: Acyl-CoA Synthetase. ACBP: Acyl-CoA Binding Protein. FABP: Fatty Acid Binding Protein. FA: fatty acid. Cn: chain of fatty acyl, Cn+2: malonyl-CoA unit addition. CPT-I: Carnitine Palmitoyltransferase I. CPT-II: Carnitine Palmitoyltransferase II. HMG-CoA: Hydroxymethylglutaryl-Coenzyme A.)

Acetyl-CoA formed is used to Krebs cycle to produce energy ATP or it is deviated to ketogenesis or cholesterol synthesis when energy supply is required. Ketogenesis is enhanced when NEFA uptake increase and when low levels of insulin action activate CPT-I; this process requires five times more acetyl-CoA than Krebs cycle to form energy, allowing the reduction of NEFA levels. When energy supply is full and glycerolipid synthesis is inhibited, cholesterol synthesis is the only way to reduce the amount of NEFA(10).

Fatty acid regulation is controlled by PPARα, SREBP-1, RXR and LXR as signal proteins. PPARα is essential to oxidation fatty acids, increasing the cellular capacity to catabolize them (high expression of FABP, FAT, CPT-I). More, *Polyunsaturated Fatty Acid* (PUFA) suppress SREBP-1 gene expression, reducing fatty acid synthesis; MUFA and *Saturated Fatty Acid* (SFA) are poor ligands. However, LXR downregulates PPARα and upregulates SREBP-1, inducing FAS and ACC expression and glycerolipid synthesis (PL and TG). Fatty acids synthesis is induced when carbohydrates, like glucose, are elevated in plasma, because insulin acts in upregulation of gene expression for synthesize lipids (10), acts in downregulation of gene expression for lipids oxidation(7) and activates glycolysis to form acetyl-CoA for Krebs Cycle(8). This insulin mechanism allows spending glucose for energy and keeps lipid reservoir for future needs.

4. Type 2 of Diabetes Mellitus, Obesity and Metabolic Syndrome

Type 2 of diabetes mellitus is a multifactorial disease, influenced by genetic and environmental factors and it is one of the major causes of mortality and morbidity, affecting 8% of the population. More, it is characterized by a chronic state of hyperglycemia, insulin resistance in tissues and compensatory hyperinsulinemia. Chronic hyperglycemia is toxic, leading to microvascular complications by the progressive accumulation of *advanced glycated end-products* (AGE) and reactive species of oxygen. Consequently, AGE lead to non-enzymatic modification of proteins and increase *glycated hemoglobin* (HbA1c) and expression of genes envolved in angiogenesis and fibrosis(22,23).

Obesity is also a major cause of morbidity and mortality, associated with an increased risk of cardiovascular diseases, metabolic syndrome and cancer; it is clinically characterized by a body mass index >30kg/m^2. Metabolic syndrome is defined by several metabolic abnormalities, including central obesity, dyslipidemia, hyperglycemia and hypertension. The prevalence of diabetes in obese patients is four times more high than normal body mass index patients(24).

4.1. Glycation and methylglyoxal

Methylglyoxal (MG) is a highly reactive dicarbonyl aldehyde which is produced during glycolysis and lipid peroxidation, a secondary metabolic compound and AGE precursor(25). Maillard reaction is a process to form AGE, by Schiff bases and Amadori products, produced from the reaction of carbonyl groups of sugar with proteins, lipids or nucleic acids. AGE result from the modification of arginine and lysine amino acids, resulting in protein denaturation(22). Several studies have reported elevated MG levels in plasma from diabetic patients (22,23) and MG adducts implicated in the macro and microvascular complications. In addition, the food with high glycemic index have a greater impact on the body particularly by MG mediated, but its pathophysiology role is not yet fully defined(25).

Furthermore, cells have enzyme systems to detoxify MG, when it is produced during metabolism of glycolysis. The glyoxalase System (GLO) is one of the most implicated glutathione-dependent processes and GLO1 overexpression protects from glucose-induced reactive oxygen species (ROS) and reduces the development of complications in several diseases. In addition, cells have other systems capable of degrading formed compounds, such as proteasome and lysosome. Besides, AGE and MG adducts are eliminated by renal excretion. Interestingly, the normalization of blood glucose in diabetic patients is not completely prevent high levels of MG in plasma, suggesting that the persistence of levels of MG are due to errors in metabolism due to accumulation of AGE and ROS production (22,25).

MG is a glycating agent, reacting with DNA, lipids and proteins, such as insulin, hemoglobin and growth factors, producing AGE. HbA1c glycated hemoglobin is a marker of glycemic control, but not by glycation MG-derived and AGE-DNA contribute to increased oxidative stress markers. Transcription factors are also strongly susceptible to be modified by the MG, influencing cellular metabolism. In the hepatocyte, as in so many other cells, oxidative stress is one of the other effects from high MG levels, increasing superoxide, hydrogen peroxide, peroxynitrite and proinflammatory cytokines and reducing the antioxidants such as glutathione, glutathione peroxidase, glutathione reductase and others (22,25).

Moreover, the formed AGE can activate specific receptors (RAGE), founded in various cells, downregulating GLO1 and activating NF-KB by NADPH oxidase, protein kinase C (PKC) and JNK, leading to the translocation of NF-κB to the nucleus. Thus, NF-κB increases the expression of adhesion molecules, vascular endothelial growth factor (VEGF), TNF-α and RAGE itself. There are also soluble RAGE (sRAGE) in plasma, which function is to reduce AGE levels in the body by preventing the tissue RAGE binding(22,25).

Finally, the MG high levels are implicated in various pathological effects such as insulin resistance and macro and microvascular complications, present in conditions such as diabetes, obesity, hypertension and atherosclerosis, may be considering an angiopathy marker. The insulin resistance may be caused by glycation of insulin or insulin receptor inactivation, decreasing IRS1 phosphorylation and PI_3K/Akt pathway. MG in macrovascular complications have been associated with endothelial damage and vascular remodeling, involving oxidative stress, decreased nitric oxide bioavailability, increased glycation and inflammation; it also occurs glycation of LDL, retaining them more in arterial walls. Regarding to microvascular complications, the MG causes a decrease in the VEGF/Angiopoietin2 ratio, which is correlated with endothelial cell apoptosis, Increased vessel permeability and decreased irrigation and hypoxia in adipose tissue(25–28).

5. Non-Alcoholic Fatty Liver Disease

Non-alcoholic fatty liver disease (NAFLD) is a pathology characterized by increased intrahepatic FFA and triglycerides. SREBP-1 is activated and enhances lipogenesis, but short-FFA (with 14 carbons), PC and plasmalogen are reduced. *Tumor Necrosis Factor* (TNF-alpha), *Tumor Growth Factor* (TGF-beta) and interleukin-6 are increased and adiponectin and leptin are decreased. More, hyperinsulinemia and reduction of apoprotein B synthesis result in hepatic lipid accumulation, with higher afflux of FFA to the liver. Several liver ligands are studied to analyze if normal functions are altered in NAFLD (see Table 1)(20).

Table 1: Liver receptors of lipid metabolism, their natural ligands, normal function and role in NAFLD (adapted from (20)*)*

Nuclear receptor	Natural ligands	Function in lipid metabolism	Function in glucose metabolism	Role in NAFLD
PPARα	Fatty acids	Regulates expression of FAS -> lipogenesis; CD36/FAT, FATPs -> FA-Uptake; Acetyl-CoA-synthetase, CPT-1 -> β-oxidation	Regulates PEPCK, GSK3, Glycogen synthase ->glycogen metabolism; insulin sensitivity	Fibrate treatment improves IR
PPARγ	Prostaglandins	Regulates expression of CD36/FAT -> FA-Uptake; SCD-1 -> FA-metabolism	Regulates GLUT-4 Expression -> insulin sensitivity	Activation; PPARγKO mice are protected from diet induced steatosis; Glitazones improve IR and TG accumulation and increase adiponectin levels

PPARδ	Fatty acids	Regulates SREBP-1c -> Lipogenesis	Induces glycolysis and pentose phosphate pathway shunt	Agonist treatment improves hepatic steatosis in mice
LXRα	Oxysterols	Regulates SREBP1c, SCD-1, FAS -> lipogenesis; cholesterol metabolism	Regulates insulin receptor expression, GLUT-4 and IRS expression -> insulin sensitivity	Induced, LXR promotes hepatic lipogenesis

Non-alcoholic Steatohepatitis (NASH) is the second step in evolution of NAFLD, involving oxidative stress, lipid peroxidation, activation of the cytochrome P450 2E1, increasing inflammatory cytokine production, activation of stellate cells and apoptosis(3).

Insulin resistance and hyperinsulinemia predispose to oxidative stress and reactive species of oxygen production by stimulating microsomal lipid peroxidases and decreasing fatty acid oxidation; peroxidases acts in PUFA, producing highly reactive aldehydic derivatives. Biopsy is necessary to differentiate NAFLD and NASH, but factors like type 2 of diabetes, increased aspartate aminotransferase (AST), TG and inflammatory cytokines and hyperinsulinemia are more associated to NASH(3).

Low levels of adiponectin are a criteria to differentiate hepatic steatosis and non-alcoholic steatohepatitis(3).

Most patients with NAFLD are asymptomatic or they have non-specific symptoms, but alanine aminotransferase (ALT) levels are often found elevated(29). Liver fat content reflects the equilibrium between FFA flux through lipolysis, fatty acid oxidation, de novo lipogenesis and VLDL production(30). This dysfunction in metabolism can increase the risk of diabetes and other diseases such as atherosclerosis and coronary artery disease (see Figure 11).

6. Lipotoxicity – hepatic insulin resistance and inflammation

The liver has an important role in lipid metabolism regulation. In fed state, the fats are stored in adipocytes and liver promotes the glycolysis for ATP formation, lipogenesis and glycogen synthesis. When energy supply is required during long non-food intake periods or exercise, stimulating lipolysis in adipocytes and gluconeogenesis and fatty acid oxidation in the hepatocyte. However, when fat intake is high and chronic, the adipocytes need the hepatocytes support to control lipidemia. Then, excess fatty acids enter in the liver, for β-oxidation, but chronicity fat diet increases insulin levels during fed phase and decrease adiponectin in obesity, inducing the lipid

synthesis in the liver and accumulating TG in lipid droplets(2). The accumulation of lipids in liver results from an imbalance among the uptake, synthesis, export and oxidation of fatty acids(31)

SFA and linoleic acid (18:2) were reported to induce inflammation by the activation of NF-κB pathway through the interaction with toll-like receptor 4 (TLR4)(32). TG accumulation in lipid droplets induces DAG formation for incorporation in VLDL vesicle, increasing DAG and ceramides and activating PKC, which activates JNK and consequently the NF-κB pathway, developing hepatic inflammation(32). Due to lipid overload, overactive oxidation and DAG lead to mitochondrial dysfunction, increasing ROS, NEFA, lipid peroxidation and more lipid droplets, as a vicious cycle. Moreover, inflammation is associated with elevated white blood cells or proinflammatory cytokines in circulation and tissue and elevated macrophage infiltration; inflammation has both beneficial and bad effects in obesity. Liver inflammation maybe is a protective mechanism against excessive lipid and glucose uptake. However, as insulin signaling is inhibited by inflammation, such mechanisms may conduce to type 2 diabetes, when chronically established.

On the other hand, lipotoxicity is another process caused by chronic and persisted elevation of FFA or NEFA, inducing obesity and insulin resistance and an increment risk for type 2 diabetes mellitus. Insulin resistance state goes along with increased adipocyte lipolysis, leading to abundant FFA in the plasma (see Figure 11). It is characterized by hyperinsulinemia, hyperglycemia in fasting condition, hyperlipidemia, impaired glucose tolerance, increased hepatic glucose production, hypoadiponectinemia and increased inflammatory markers in plasma and it occurs many years before open type 2 of diabetes mellitus(32).

Adiponectin is a protein expressed in adipocytes due to the LPL activity, removing the NEFA and integrating them within the adipocytes. This increase allows the binding with nuclear receptor PPARγ and RXR, stimulating adiponectin expression and releasing into the blood. Adiponectin is inhibited in inflammatory process, increased cAMP and insulin signal(33). The liver has adiponectin receptor, adipoR, and its function is to activate AMPK and PPARα, increasing the uptake and oxidation of glucose and lipids(34). This molecule has the ability to inhibit directly lipogenesis enzymes of fatty acids and forward to mitochondrion to increase oxidation. Therefore, the adiponectin has an important role in the oxidation, preventing synthesis of fatty acids, hepatic TG accumulation and inhibiting oxidative stress and inflammation. In other hand, adiponectin is decreased in obese and type 2 diabetic patients, inducing lipotoxicity and insulin resistance. It has been associated with insulin sensitivity and has anti-inflammatory effects(3,24,33).

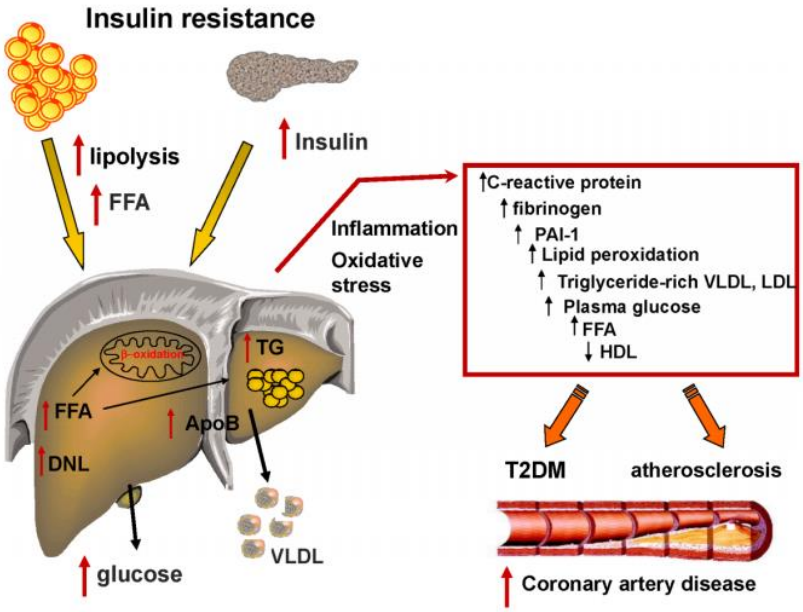

Figure 11: Interaction of insulin resistance and lipotoxicity(30)

7. Overall mechanism of glycation and lipotoxicity

Hepatic Steatosis result in an accumulation of lipid droplets and alterations of β-oxidation, and fatty acid and VLDL synthesis. Low levels of PPARα lead to hepatic steatosis(10) and insulin resistance(35) due to decreased oxidation. On the other hand, SREBP-1 and ACC are markedly elevated due to hyperinsulinemia, contributing to de novo fatty acids synthesis(10). In this situation, when adipocytes achieved triglycerides store threshold, they release fatty acids to the plasma which will further increased the lipid load to the liver. Glycerophosphate acyltransferase, lysophosphatidate acyltransferase and diacylglycerol acyltransferase are the enzymes responsible to triacylglycerol synthesis and accumulation in liver. The progression of insulin resistance starts in peripheral tissue such as alteration of lipolysis in adipose tissue and hyperinsulinemia. The consequent influx of fatty acids to the liver and increased hepatic TG finally hepatic insulin resistance(35).

TG accumulates as lipid droplets in liver or are incorporated and exported in VLDL particles (Figure 11). When accumulated as NEFA or secondary metabolites such as ceramides and DAG they induce inflammation through activation of stress pathways. Moreover, SFA activates the TLR4 and excessive NEFA induce reticulum endoplasmic stress by phosphorylation of protein kinase R-like endoplasmic reticulum kinase (PERK). Regarding phospholipids, elevated LPC levels are also associated to lipotoxicity marker in NASH due to inflammation that remove one fatty acid in PC molecules, but its levels are proportional to disease severity(36).

CHAPTER 2

AIMS

Aims

The majority of patients with type 2 diabetes is clinically characterized by insulin resistance and obesity, increasing the risk of developing fatty liver and non-alcoholic fatty liver disease; with this work, it was intended to use an animal model – Wistar Rats – with administration of methylglyoxal and high-fat diet for induction of glycation and obesity, respectively.

The objectives of this work are to understand the role of glycation induced by methylglyoxal in the alteration of lipid metabolism in obesity and to know the implications of such mechanisms in local and systemic parameters of glucose metabolism. In this way, the lipid liver analysis was performed by different approaches: lipidomic techniques and magnetic resonance. More, it was necessary to correlate these results with the evaluation of liver pathways of the lipid metabolism and the insulin signaling.

At the end of the project will be possible to understand better how glycation and high-fat diet can induce glucose and lipid dysmetabolism, insulin resistance and lipotoxicity and consequently non-alcoholic fatty liver disease.

CHAPTER 3

MATERIALS AND METHODS

Materials and Methods

1. Materials

1.1. Reagents

Salts and organic solvents used in solution preparations were purchased to Sigma Chemicals (United States of America - USA) or Merck Darmstad (Germany), with the highest grade of purity commercially available. Perchloric acid from Panreac (Barcelona, Spain). Aceto-nitrile, chloroform, methanol and hexane from Fisher scientific (Leicestershire, UK). The water was of MilliQ purity filtered through a 0.22-mm filter (Milipore, USA).

1.2. Other materials

During the experiments, it was necessary to use common materials like horizontal shaker (model DSR 2800V, Digisystem Lab. Instruments Inc, Thailand), electronic and scale and precision scale (Precisa 80ª-200M and Libra EB-2800, Japan), centrifuge (Thermo Electron Corporation, USA), glucometer (Bayer SA, Portugal), homogenizer (model A TM, FLAC Instruments, Italy), microplate reader (Gen5 Software, Biotek Instruments Inc, USA), pH reader (MicropH, Crison, Spain), automatic micropipettes (Gilson medical Electronics, France), microplates (Immuno plate maxisorp C96, Nunc Roshild, Denmark), pipette tips (Gilson medical Electronics, France), potter and piston (F28D03, Thomas Scientific, USA), ELISA software (Gen5, Biotek Instruments Inc, USA), glucometer strips (Bayer SA, Portugal), blood collection tubes (BDVacutainer, United Kingdom - UK), vortex (UNIMAG, ZX, Germany), extraction and quantification tubes, cap and spares (11ml, 16x100 mm, PYREX, Scilabware, UK).

2. Animals and Treatments

Wistar rats were obtained from the breeding colony at the Faculty of Medicine, University of Coimbra and they were kept under controlled ventilation, temperature (22-24ºC), humidity (50-60%) and light (12h light/ 12h darkness) with free access to water and food. Local Institutional Animal Care and Use Committee (ORBEA IBILI-FMUC) approved the experimental protocol and all the procedures were performed by licensed users (FELASA). 8 month old male Wistar rats were divided in four groups (n=12/group): Control (Ct) with standard diet AO3 (5% of triglycerides and 45% of carbohydrates, SAFE, France); Methylglyoxal group (MG) with standard diet and MG administration; High-fat diet-fed group (HFD) with a high-triglyceride diet; High-fat diet with MG combination group (HFDMG).

High-fat (HF) diet has 40% of triglycerides and 10% of carbohydrates (231 HF, SAFE, France) and it was administered during 18 weeks from 8 to 12 months old. Methylglyoxal (Sigma, USA) was diluted in the daily water (100 mg/Kg/day) with weekly adjustments according to the body weight.

This experimental protocol was described and optimized by Laboratory of Physiology, Institute of Biomedical Imaging and Life Sciences (IBILI), Faculty of Medicine, University of Coimbra, Portugal(26,37).

Standard diet and high fat diet were analyzed by gas chromatography(38) to identify and quantify different species of esterified fatty acyl chains. 50mg of each diet was prepared with a methanolic solution of potassium hydroxide (2M) according to a referenced method. Only 10mg of standard diet and 10mg of high fat diet were diluted in 100μl and 650μl, respectively, of hexane solution containing methylated fatty acids and 3μl of each sample was injected in the gas chromatograph. Fatty acyl chain with 17 carbons (C17 – 7.5μg) was used as internal standard. The GC injection port was programmed at 523.15 K and the detector at 543.15 K. Oven temperature was programmed as follows: initially stayed 3 minutes at 323.15 K, raised to 453.15 K (25 K min^{-1}), held isothermal for 6 minutes, with a subsequent in-crease to 533.15 K (40 K min^{-1}) and maintained there for 3 minutes, performing 19 minutes totally. The carrier gas was hydrogen flowing at 1.7 mL/min. The gas chromatograph (Clarus 400, PerkinElmer, Inc. USA) was equipped with DB-1 column with 30 m length, 0.25 mm internal diameter and 0.15lm film thickness (J&W Scien-tific, Agilent Technologies, Folsom, CA, USA) and a flame ionization detector.

3. In vivo Analysis

3.1. Body Weight and Glycemic Levels

Body weight was registered during the treatment at the beginning, at 4, 8 and 14 weeks and at the end of treatment. HbA1c level, fasting (fasting blood sugar test) and 1h and 2 hours glycemia after intraperitoneal glucose administration (1.8 g/Kg) were measured in the tail vein in overnight (18h) fasted rats.

3.2. Lipid Levels Determination – Magnetic Resonance Spectroscopy

A high-resolution magic-angle spinning ^{1}H nuclear magnetic resonance (NMR) spectroscopy of liver tissues coupled with principal components analysis were performed using a BioSpec 9.4 T MRI scanner (Bruker Biospin, Ettlingen, Germany). Rats (n=6/group) were kept anesthetized by isoflurane (2-3%) with 100% O_2 with body temperature (37ºC) and respiration monitoring (SA Intruments SA, Stony Brook, USA). Water-suppressed ^{1}H NMR liver lipid spectrums were analyzed

using homemade software implemented in Matlab (v2013a, Mathworks) to obtain hepatic lipid signals. This experimental protocol was described and optimized by Institute of Nuclear Sciences Applied to Health, ICNAS, University of Coimbra, Portugal(39).

4. Sample Collections

4.1. Blood

Blood samples were collected by cardiac puncture after 16-18 hours fasting in anesthetized rats with intraperitoneal injection of ketamine chloride (75 mg/kg, Parke-Davis, Ann Arbor, USA) and chlorpromazine chloride (2.65 mg/kg, Lab. Vitória, Portugal). Serum and plasma were collected in BD Vacutainer tube and BD Vacutainer K3E, respectively, with EDTA (5,4mg); then, they were centrifuged (2500 RPM, 4ºC, 10 minutes) and stored in aliquots at -20ºC.

Systemic Parameters were determined in fasted rat blood samples. Serum triglyceride levels were determined using commercial kits (Olympus-Diagnóstica, Portugal, Produtos de Diagnóstico SA, Portugal). Plasma levels of free fatty acids were assessed spectrophotometrically using the FFA Assay Kit (ZenBio, NC, USA). Plasma insulin levels were determined using the Rat Insulin ELISA Kit (Mercodia, Sweden). Serum concentration of adiponectin was determined using the Rat Adiponectin Immunoassay Kit (Invitrogen, USA). Plasma levels of total cholesterol, HDL cholesterol, total protein, albumin, alanine aminotransferase (ALT), aspartate aminotransferase (AST), alkaline phosphatase, gamma glutamyl transferase (GGT) and total bilirubin were measured at Clinical Pathology Service in Centro Hospitalar Universitário de Coimbra, Portugal.

4.2. Liver

After the sacrifice by cervical displacement, liver tissues were harvested, weighed and washed in isotonic solution (0,9% NaCl); before freezing at -80ºC, livers were photographed with a no filters camera (Exilim, Casio, Japan).

4.2.1 Western Blotting

Hepatic protein determination was performed by homogenization of liver tissue (50mg) (n=6) in 2ml of buffer (25 mM Tris, 150 mM NaCl, 1% Triton X-100, 1 mM EDTA, 1 mM EGTA, 10 mM PMSF and 40 μl/g tissue of proteases inhibitor cocktail (Sigma, USA), pH = 7.7) and centrifuged at 14000xg, 20 minutes, 4ºC. Protein concentration was determined using the BCA method (Pierce, USA).

Liver samples were separated by SDS-PAGE and transferred to PVDF membranes. Membranes were blocked with TBST solution (25mM Tris-HCl, 150mM NaCl, 0.1% Tween, pH=7.6, 5% BSA) and incubated overnight at 4ºC with the respective primary antibody (see Table 2) and during 2 hours at room temperature with the secondary antibody (anti-mouse, GE Healthcare, UK; anti-rabbit and anti-goat, Bio-Rad, USA). Membranes were revealed using ECL substrate in a Versadoc system (Bio-Rad, USA) and analyzed with Image Quant® (Molecular Dynamics, USA).

Table 2: List of primary antibodies for lipid oxidation and insulin signaling

Primary Antibodies
Calnexin (AB0037, Sicgen, Portugal)
AKT, p(Ser473)AKT, AMPK, p(Thr172)AMPK, ACC and p(Ser79)ACC (#9272, #4058, #2532, #2535, #3676 and #3661, Cell Signaling, USA)
F4/80 and GLUT2 (ab74383 and ab54460, Abcam, UK)
IRβ and p(Tyr1163)IRβ (sc-57342 and sc-25103, Santa Cruz Biotechnology, EUA)

4.2.2 Lipidomic Approaches

Hepatic lipid levels were determined by different lipidomic approaches (n=3). Liver tissue was homogenized in phosphate buffer saline (PBS), pH 7.4 and lipid extraction was performed by Folch Method(40), using a chloroform:methanol (2:1 v/v) solution.

Total phospholipid (PL) quantification was measured by colorimetric phosphorous assay, after perchloric acid digestion at 180ºC, as described before(41). Phospholipid internal standards (see Table 3) were purchased to Avanti Polar Lipids, Inc. (Alabaster, AL, USA).

Phosphorous assay was performed to calculate the amount of each PL class after thin layer chromatography (TLC) separation in 60μg of total PL. TLC uses a silica gel plates with a concentrating zone of 2.5 x 20 cm (Merck, Darmstadt, Germany) and it was developed with chloroform/ethanol/water/triethylamine solvent mixture (35:30:7:35, v/v/v/v)(42). Lipid spots were visualized with UV (λ= 254 nm) after detection with primuline (Sigma, St Louis, MO, USA) and PL classes were identified by internal standards (see Table 3).

Phospholipids (PL) and triglycerides (TG) were detected by mass spectrometry (MS) after separation by high performance liquid chromatography (HPLC). HPLC system (Waters Alliance 2690) was used with an Ascentis Si column (15 cm x 1 mm, 3lm) and a pre-column split (Acurate, LC Packings, USA) in order to obtain a flow rate of 20μL min^{-1}.

The solvent system consisted in two mobile phases as follows: mobile phase A (acetonitrile:methanol:water; 55:35:10 (v/v/v) with 1 mM ammonium acetate) and mobile phase B (acetonitrile:methanol 60:40 (v/v) with 1 mM ammonium acetate). Initially, 0% mobile phase A was held isocratically for 8 minutes followed by linear increase to 60% of A within 7 minutes and maintained for 40 minutes. Samples (20μg of total phospholipid) were separated by HPLC, which was coupled to a linear ion trap (LXQ; Thermo Finnigan, San Jose, CA, USA) mass spectrometer. The LXQ were operated in both positive (electrospray voltage +5 kV) and negative (electrospray voltage -4.7 kV) with 275ºC capillary temperature and the sheath gas flow of 8 U. Normalized collision energy™ (CE) varied between 20 and 27 (arbitrary units) for MS/MS.

Data acquisition was carried out on an Xcalibur data system (V2.0). Relative quantitation of individual phospholipid species were determined by the ratio between the area of reconstructed ion chromatogram of a given m/z value against the area of the reconstructed ion chromatogram of the respective class and absolute by internal standards (see Table 3).

Table 3: List of phospholipid internal standards

CL	1',3'-bis[1,2-dimyristoyl-sn-glycero-3-phospho]-sn-glycerol	m/z 1239.4 $[M+H]^-$	1.51μg	**CL**
dMPC	1,2-dimyristoyl-sn-glycero-3-phosphocholine	m/z 736.2+58 $[M+CH_3COO]^-$	5 μg	**PC**
LPC	1-nonadecanoyl-2-hydroxy-sn-glycero-3-phosphocholine	m/z 596.2+58 $[M+CH_3COO]^-$	1.49μg	**LPC**
dMPE	1,2-dimyristoyl-sn-glycero-3-phosphoethanolamine	634.5 $[M+H]^-$	2.5μg	**PE**
dMPA	1,2- dimyristoyl-sn-glycero-3-phosphate	591.3 $[M+H]^-$	1.5μg	**PA**
dMPG	1,2-dimyristoyl-sn-glycero-3-phospho-(1'-rac-glycerol)	665.5 $[M+H]^-$	1.5μg	**PG**
dMPS	1,2-dimyristoyl-sn-glycero-3-phospho-L-serine	678.3 $[M+H]^-$	1.5μg	**PS**
dPPI	1,2-dipalmitoyl-sn-glyce-ro-3-phospho-(1'-myo-inositol)	No standard		**PI**

MS data presented by means of relative abundance per class and, depending on the phospholipid classes, the spectra were analyzed in positive or negative ion modes. Triglycerides

were analyzed in the positive ion mode and phospholipids: lysophosphatidylcholines (LPC), phosphatidylcholines (PC), sphingomyelins (SM), phosphatidylethanolamines (PE), cardiolipins (CL), phosphatidylserines (PS), phosphatidylinositols (PI), phosphatidylglycerol (PG) and phosphatidic acid (PA) were analyzed in negative ion modes. MS/MS was performed for each ion to identify and confirm their structure, according to the typical fragmentation pathways(43), LIPID MAPS(44) and LIPID Mass Spec. Prediction program(v1.5, LIPID MAPS, 2009)(44).

Total of esterified fatty acyl were measured by gas chromatography (GC) after transesterification of lipid liver extracts (approximately 90μg of total PL), with controlled dilutions in highest fat liver lipid samples and 2μl was injected in gas chromatograph. C17 was used as internal standard as mentioned above.

5. Statistical Analysis

Results are presented as mean and standard error of the mean (SEM) for each experimental group and non-parametric Kruskal-Wallis test was applied to determine statistical differences between the groups, using SPSS software (IBM, NY, USA). p values <0.05 were considered to be statistically significant.

CHAPTER 4

RESULTS

Results

1. Body Weight, food, liver weight, macroscopy and hepatic function test

The body weight after the four months of treatment shows an increase in rats with high fat diet administration (HFD group), but not in the HFDMG group, showing an inhibitory effect of methylglyoxal weight gain (HFDMG group) administration (Figure 12).

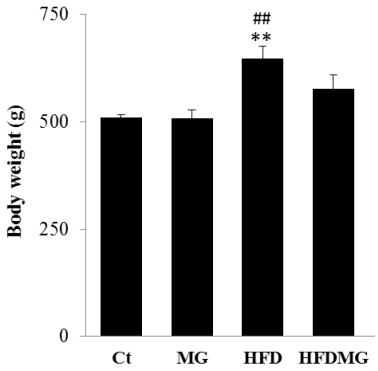

*Figure 12: Body weight in the end of the treatment. *different from Ct. # different from MG. 1 symbol p<0.05. 2 symbols p<0.01.*

*Table 4: Food consumed during the treatment, liver weight and hepatic function test. *different from Ct. # different from MG. 1 symbol p<0.05.*

Group	Ct	MG	HFD	HFDMG
Food (g/rat/day)	22.90 ± 0.70	24.30 ± 1.60	15.10 ± 1.10 **##	14.40 ± 0.70 **##
Liver weight (g)	13.90 ± 0.62	12.41 ± 0.58	13.37 ± 0.69	13.91 ± 0.67
Total Protein (g/dl)	6.41 ± 0.10	6.18 ± 0.05	6.02 ± 0.15	6.10 ± 0.07
Albumin (g/dl)	2.78 ± 0.07	2.85 ± 0.03	2.62 ± 0.09	2.47 ± 0.07 **#
AST (U/l)	188.00 ± 30.87	141.50 ± 15.18	162.67 ± 27.40	162.86 ± 21.24
ALT (U/l)	71.54 ± 9.93	58.00 ± 8.28	72.83 ± 11.56	63.14 ± 14.79
Alkaline Phosphatase (U/l)	81.00 ± 8.95	82.50 ± 15.16	101.00 ± 13.78	82.29 ± 25.34
GGT (U/l)	1.00 ± 0.11	1.00 ± 0.00	1.17 ± 0.17	1.00 ± 0.00
Total Bilirubin (mg/dl)	0.10 ± 0.01	0.10 ± 0.00	0.08 ± 0.02	0.11 ± 0.03

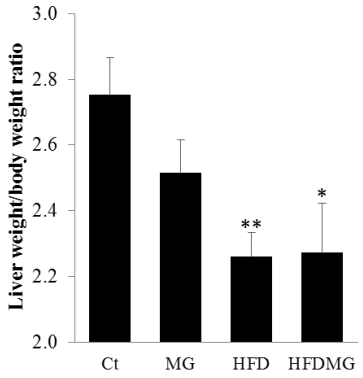

*Figure 13: Liver weight/body weight ratio. *different from Ct. 1 symbol p<0.05. 2 symbols p<0.01.*

In Figure 13 it can be also noted that the ratio between liver and body weight decreased in the groups with fat diet administration (HFD and HFDMG groups), with greater statistical significance in the HFD group.

The HFD and HFDMG groups ate the same amount of fat diet during the treatment. The size of the liver was also not different to the control group, decreasing the ratio between the body weight and liver (Table 4).

In liver function tests, there was no difference in total protein levels, liver enzymes and bilirubin. It only was observed a statistically significant decrease in plasma levels of albumin in HFDMG group (Table 4).

After the analysis of fatty acids from diets by GC-FID, it was found that the standard diet has less amount of fatty acids and is more rich in PUFA (18:2). On the other hand, fat diet is much more rich in fatty acids (in species and amount), especially in MUFA (18:1) and SFA (16:0 and 18:0). Fat diet has also high levels of essential fatty acid 18:2 (linoleic acid) (Table 5).

Table 5: Fatty acid species from standard and high-fat diet and respective amount per gram of diet (mg/g), by GC-FID.

Fatty Acid		Standard Diet	High-fat Diet
14:0	Myristic	-	0.312
16:1	Palmitoleic	-	0.702
16:0	Palmitic	0.251	7.058
18:2	Linoleic	0.511	4.224
18:1	Oleic	0.177	11.698
18:0	Stearic	-	2.539
Total		0.940	26.533

Macroscopy analysis of the appearance of the liver shortly after the sacrifice showed visible lipid accumulation in HFD and HFDMG groups (Figure 14).

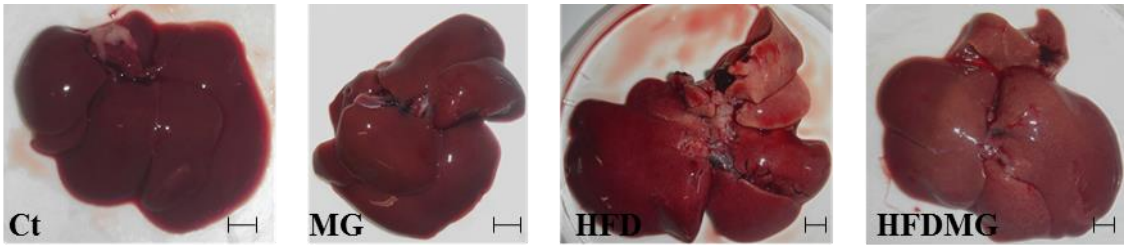

Figure 14: Macroscopic visualization of a representative liver for each group. ├┤ scale 2cm

2. *In vivo* magnetic resonance spectroscopy

At the end of treatment and days prior to sacrifice, rats performed a non-invasive technique of magnetic resonance imaging to analyze the liver and the amount of fat by ^{1}H spectroscopy, in which each peak corresponds to a different environment proton in the same molecule (Figure 15).

Phospholipids do not vibrate in the same way as the cytosolic lipids, so the signals received by NMR are only the cytosolic lipids (TG and DAG) and not the membrane lipids(45).

After obtaining data and peak values, it was used the already pre-established equations to determine values of the lipid fraction and saturated, unsaturated, mono and polyunsaturated fractions(45).

Considering the previous results of Figure 13, Figure 14 and Table 5, it is possible to confirm the results with this *in vivo* technique.

^{1}H chemical shift (ppm)	Molecule	Assignment
0.89–0.95	Lipids	$C\underline{H}_3$–$(CH_2)_n$–
0.96 (t)	ω-3-Type of fatty acid	$C\underline{H}_3$–CH_2–CH=CH
1.28–1.39	Lipids	CH_3–$(C\underline{H}_2)_n$–
1.51 (d)	Alanine	β–$C\underline{H}_3$
1.61	Lipids	–$C\underline{H}_2$–CH_2–C=O
2.07	Lipids	–$C\underline{H}_2$–CH=CH–
2.25	Lipids	–CH_2–$C\underline{H}_2$–C=O
2.78	Lipids	=CH–$C\underline{H}_2$–CH=
3.22	Choline/ phosphocholine	$N^+(C\underline{H}_3)_3$
3.24–3.27	Taurine/TMAO	–$C\underline{H}_2SO_3$/$C\underline{H}_3$
3.42	Taurine	–$C\underline{H}_2NH_2$
3.35–4.03	Glucose/glycogen	$\underline{H}_2$–$\underline{H}_5$, ring protons
4.11/4.32	Triglyceride	–$C\underline{H}_2$–O–COR
5.24 (d)	α-Glucose	C1$\underline{H}$
5.25	Triglyceride	–$C\underline{H}$–O–COR
5.3–5.35	Lipids	–$C\underline{H}$=$C\underline{H}$–
5.38–5.42	Glycogen	C1$\underline{H}$

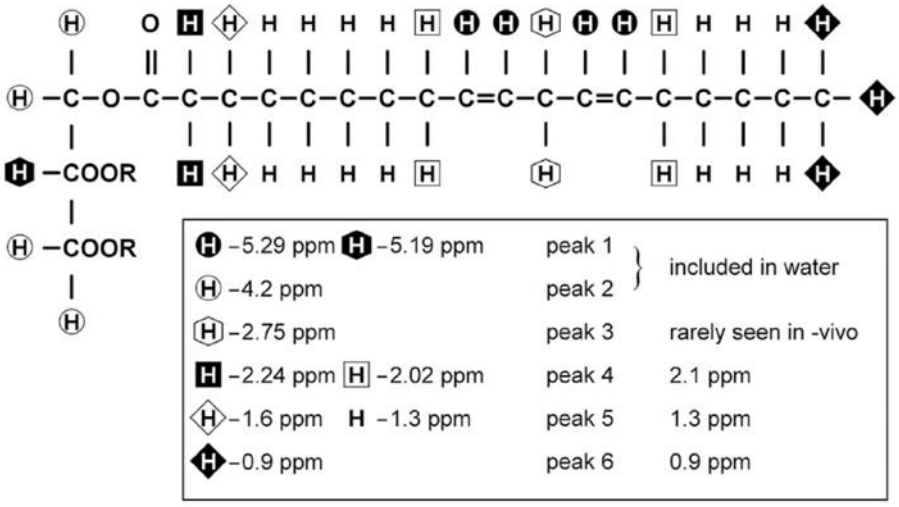

Figure 15: adapted figure of ^{1}H NMR assignments for control rat liver tissue (39) *and diagrammatic representation of typical glycerolipid molecule*(46). *Fatty acyl chain represents linoleic acid (18:2), R represents other fatty acyl chain or hydrogen. Each type of proton has different chemical shift (ppm) and peak in resonance spectrum.*

The lipid fraction increased in the HFD and HFDMG group, while the unsaturated fraction decreases and saturated fraction increases over the groups, with a significant difference more evident only in the HFDMG group (Figure 16).

Although the unsaturated fraction is decreasing, polyunsaturated fraction decreases in the groups with administration fat diet (HFD and HFDMG groups) and monounsaturated fraction have

a trend to increases due to the high concentration of oleic acid (18: 1) in the high-fat diet (Figure 16).

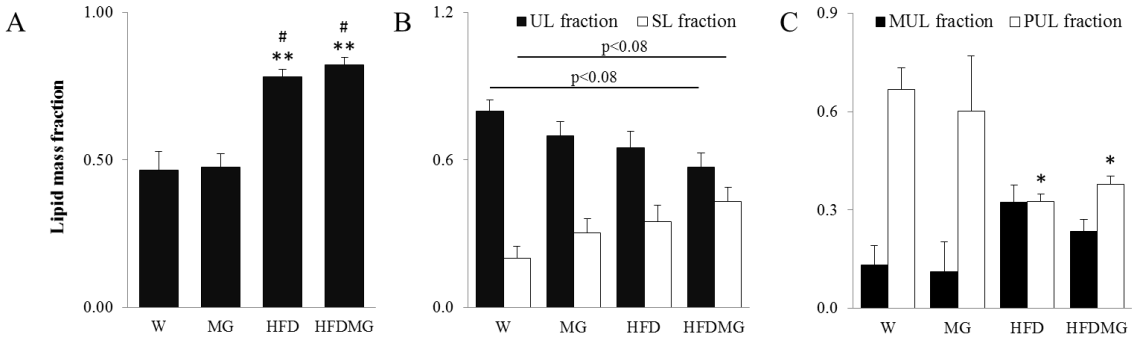

Figure 16: Liver lipid mass fraction (A), unsaturated (UL) and saturated (SL) (B) and monounsaturated (MUL) and polyunsaturated (PUL) (C) lipid fractions, international units, (equations calculated from (45)*). *different from Ct. # different from MG. 1 symbol p<0.05, 2 symbols p<0.01.*

Besides this, the formula for identifying DAG and fatty acids was never described, mainly the inability of the MRI used in previous studies to separate 5.19 ppm signal corresponding to an identifier of glycerol (isolated proton) and the proton signal 5.29 ppm of double bonds between carbons (Figure 15).

However, the magnetic resonance imaging machine used at ICNAS has a 9 Tesla magnet and it can isolate the peak 5.19 ppm. Thus, it was possible to calculate the percentage of esterification of glycerol, by the ratio 2.24ppm x (2/6)/5.19ppm, and the levels of NEFA, by the ratio of 0.9ppm x (3/9)/5.19ppm. Results reveal a decreasing esterification of glycerol and an increasing ratio of the fatty acid/glycerol in HFDMG group compared to the control group, suggesting an increase of non-esterified fatty acids (fatty acids from phospholipids not include) (Figure 17).

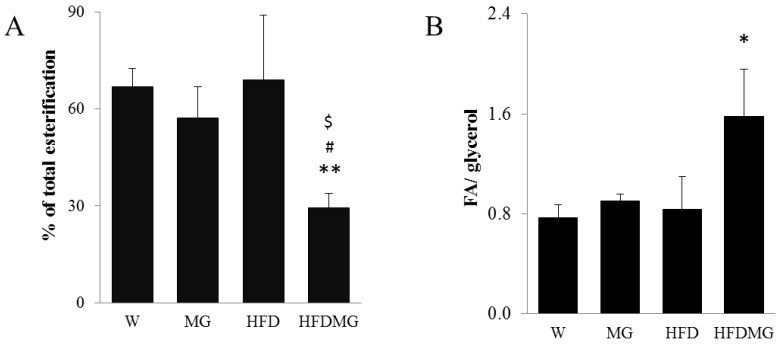

*Figure 17: Percentage of total esterification (A) and FA/glycerol ratio (B). *different from Ct. # different from MG. $ different from HFD. 1 symbol p<0.05, 2 symbols p<0.01.*

3. Lipidomic analysis

3.1. Analysis of liver trigycerides content

Liver triglycerides (TG) quantities were obtained in the positive mode complexed with ammonia (+17 NH_3), showing increasing trend in the groups with fat diet administration, despite the HFDMG group has a very large deviation (Figure 18).

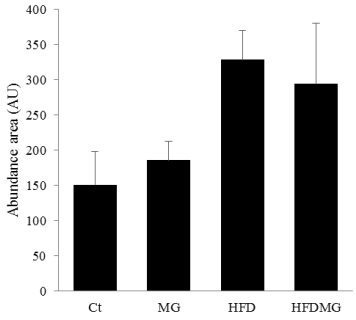

Figure 18: Total amount of TG in units of the area of reconstructed ion chromatogram (UA) by HPLC-MS/MS.

The species containing the fatty acid 18:1 were elevated mainly in the HFD group. Moreover, TGs rich in 20:4 (TG-858, TG-868 and TG-894) were decreased in HFD and HFDMG groups. So, statistically significant alterations of TG are mainly present in the HFD group (Figure 19). Table 6 lists up all identified species of TG, quantification and the constituent fatty acids. The most abundant TG are TG-870, TG-872, TG-874, TG-896, TG-898, TG-900, TG-920 and TG-922.

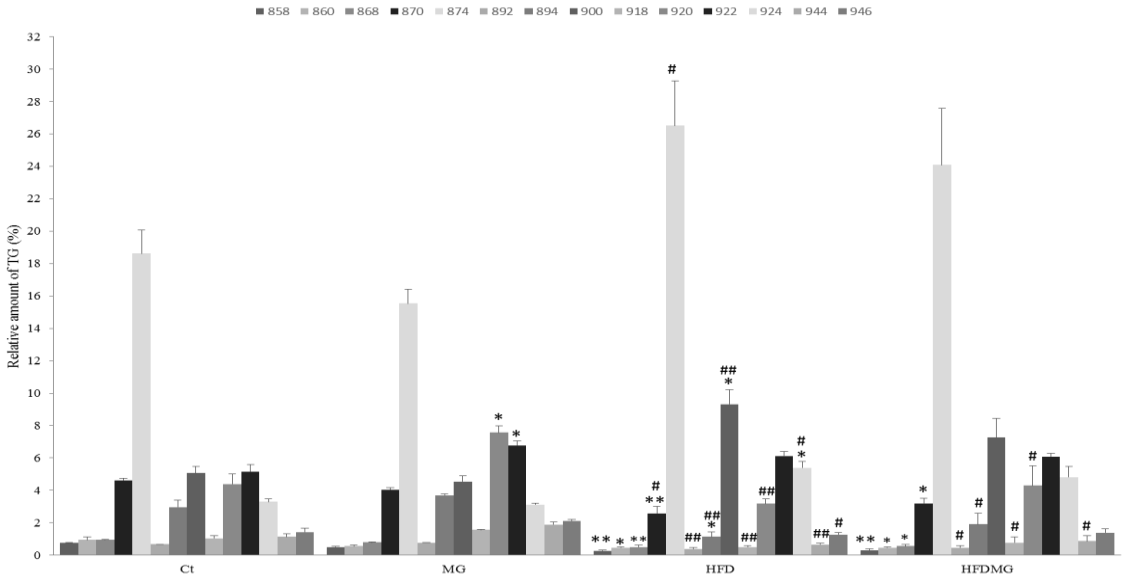

*Figure 19: Relative amount of TG with statistically significant difference, by HPLC-MS/MS. *different from Ct. # different from MG. 1 symbol p<0.05, 2 symbols p<0.01*

*Table 6: Relative amount of different species of TG ($[M+NH_3]^+$), with respective fatty acid constitution and statistical p-value, by HPLC-MS/MS. *(carbons number/double bounds). ** identified fatty acids in MS/MS. *** less abundant fatty acids.*

m/z	Species	Ct	MG	HFD	HFDMG	p-value
842	(50:5)*	0.36± 0.04	0.34±0.03	0.22± 0.08	0.23±0.07	-
844	(50:4)*	1.24± 0.22	0.97±0.08	0.69± 0.13	0.81±0.18	-
846	16:0/16:1/18:2	2.92± 1.21	1.66±0.15	1.73± 0.18	1.94±0.14	-
848	16:0/16:0/18:2**	4.71± 2.45	2.33±0.14	3.37± 0.32	2.96±0.22	-
858	O-16:0/16:0/20:4	0.75± 0.02	0.51±0.03	0.27± 0.07	0.31±0.08	p<0.05
860	O-16:0/18:1/18:2 O-18:1/16:1/18:1	0.95± 0.16	0.57±0.05	0.46± 0.06	0.46±0.04	p<0.05
862	O-16:0/18:0/18:2 O-16:0/18:1/18:1	0.78± 0.25	0.42±0.07	0.46± 0.01	0.41±0.02	-
868	20:4/16:1/16:1	0.94± 0.03	0.79±0.03	0.50± 0.15	0.56±0.12	p<0.05
870	18:2/18:2/16:1**	4.63± 0.12	4.05±0.13	2.57± 0.43	3.18±0.33	p<0.05
872	16:0/18:2/18:2**	18.81± 1.56	18.96±0.60	14.85± 1.18	16.99±0.56	-
874	18:2/18:1/16:1**	18.61± 1.47	15.54±0.89	26.50± 2.75	24.08±3.49	p<0.05
892	16:1/16:1/22:6 O-18:0/18:0/18:1	0.68± 0.00	0.78±0.01	0.38± 0.08	0.46±0.14	p<0.05
894	16:0/16:1/22:6 18:2/20:4/16:1 O-18:0/18:0/18:0	2.97± 0.43	3.69±0.10	1.15± 0.28	1.91±0.70	p<0.05
896	18:2/20:4/16:0**	7.53± 0.93	8.84±0.29	6.25± 0.46	6.51±0.75	-
898	16:0/20:4/18:0** 18:1/18:2/18:2**	7.80± 0.82	7.78±0.40	10.12± 0.34	8.98±0.74	-
900	16:0/18:0/20:4** 18:1/18:1/18:2** 18:0/18:2/18:2**	5.06± 0.42	4.54±0.36	9.32± 0.90	7.26±1.19	p<0.05
918	16:1/18:2/22:6 16:1/20:4/20:4	1.04± 0.15	1.56±0.04	0.51± 0.08	0.78±0.33	p<0.05
920	16:0/18:2/22:6 16:0/20:4/20:4	4.39± 0.62	7.57±0.41	3.18± 0.31	4.28±1.23	p<0.05
922	16:0/18:1/22:6 16:1/18:0/22:6 28:1/18:2/20:4	5.16± 0.42	6.78±0.26	6.11± 0.31	6.08±0.21	p<0.05
924	16:0/18:0/22.6** 18:1/18:1/20:4** 18:0/18:2/20:4**	3.29± 0.19	3.11±0.08	5.39± 0.40	4.82±0.65	p<0.05
934	18:0/18:2/22:6 O-18:0/20:4/20:4 O-18:1/18:1/22:6	0.57± 0.04	0.53±0.02	0.27± 0.04	0.37±0.14	-
944	16:0/20:4/22:6 18:2/18:2/22:6 18:2/20:4/20:4	1.14± 0.19	1.89±0.16	0.65± 0.11	0.88±0.33	p<0.05
946	18:1/18:2/22:6 18:1/20:4/20:4	1.42± 0.25	2.12±0.09	1.28± 0.12	1.39±0.25	p<0.05
948	18:2/18:0/22:6 18:0/20:4/20:4 18:1/18:1/22:6	1.30± 0.18	1.56±0.07	1.62± 0.07	1.43±0.05	-
950	18:1/18:0/22:6	0.97± 0.10	0.82±0.28	0.60± 0.34	1.06±0.23	-
960	18:0/10:4/22:5***	0.22± 0.03	0.24±0.05	0.15± 0.04	0.17±0.06	-
962	(58:1)*	0.21± 0.02	0.24±0.04	0.15± 0.03	0.18±0.05	-
968	22:6/20:4/18:2 16:0/22:6/22:6	0.37± 0.02	0.55±0.04	0.26± 0.05	0.36±0.16	-
970	18:1/20:4/22:6	0.42± 0.04	0.52±0.03	0.36± 0.08	0.42±0.09	-
972	18:0/20:4/22:6	0.49± 0.06	0.49±0.04	0.45± 0.06	0.47±0.03	-
974	18:0/20:4/22:5	0.27± 0.01	0.28±0.04	0.22± 0.03	0.25±0.04	-

3.2. Analysis of liver fatty acid content

In the sample analysis by GC-FID, it was possible to identify and quantify esterified fatty acids (in PL, TG, DAG and cholesterol esters). The total amount of esterified fatty acids was significantly increased in HFD group, but not in HFDMG group. Together with data from magnetic resonance informing increased lipid (fatty acid) fraction in HFD and HFDMG group, this suggests increased NEFA in HFDMG group (Figure 16A, Figure 17A and Figure 20B). The most abundant fatty acids in the esterified pool are palmitic acid (16:0), stearic acid (18:0), oleic acid (18:1), linoleic acid (18:2), arachidonic acid (20:4) and docosahexaenoic acid (22:6) (Figure 20A). The fatty acids 16:0 and 18:2 did not change between groups, but HFD and HFDMG groups had decreased PUFA 20:4 and 22:6. Importantly, the HFD group, but not the HFDMG group, had significantly decreased levels of 18:0 and increased 18:1. The sum of the different fatty acids resulted in increased total unsaturated fatty acids in HFD group, due to increased monounsaturated ones, also resulting in increased unsaturated/saturated fatty acid ratio (Figure 20C and D). HFDMG group showed a more modest increase of monounsaturated fatty acids, resulting in an unsaturated/saturared fatty acid ratio similar to control rats, despite the increase of total lipid mass (Figure 20C and D).

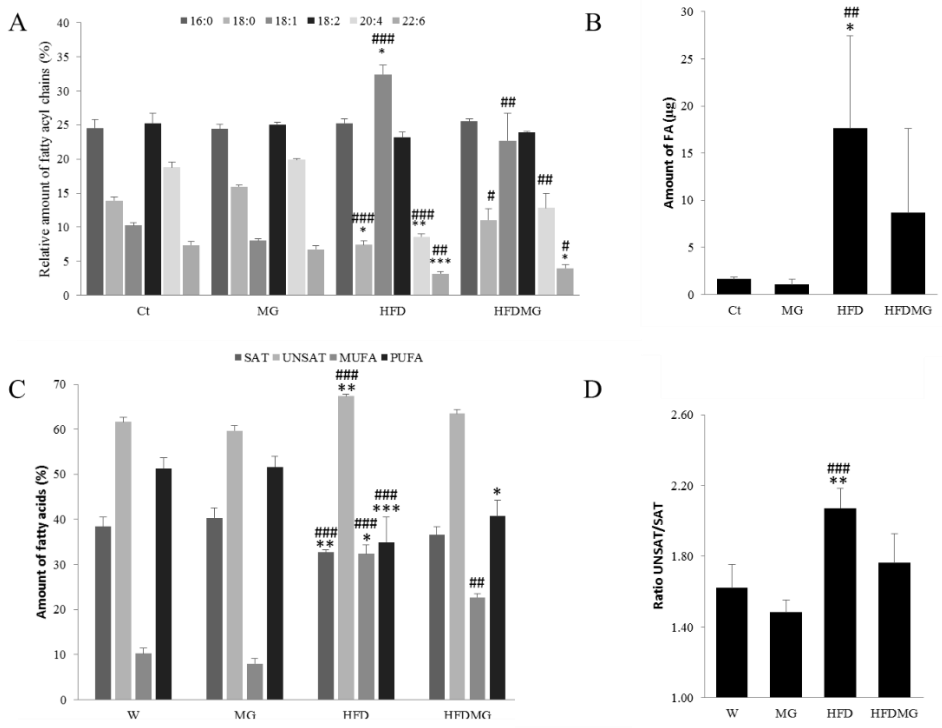

*Figure 20: Relative percentage of esterified liver FA present in total lipid extracts per group (A) and total amount (B) by GC-FID. Relative percentage of saturated (SAT), unsaturated (UNSAT), monounsaturated (MUFA) and polyunsaturated (PUFA) fatty acids (C). Unsaturated/saturated ratio (D). *different from Ct. # different from MG. 1 symbol p<0.05, 2 symbols p<0.01, 3 symbols p<0.001.*

3.3. Analysis of liver phospholipid profile

Lipidomic techniques allowed to analyze liver samples after extraction of lipids, identifying and quantifying TG and esterified fatty acids, but also PL. The total amount of PL per gram of liver had no significant variations per group, but after separation by TLC and HPLC-MS/MS, all PL classes were quantified and observed statistically significant differences in some classes of PL (Figure 21).

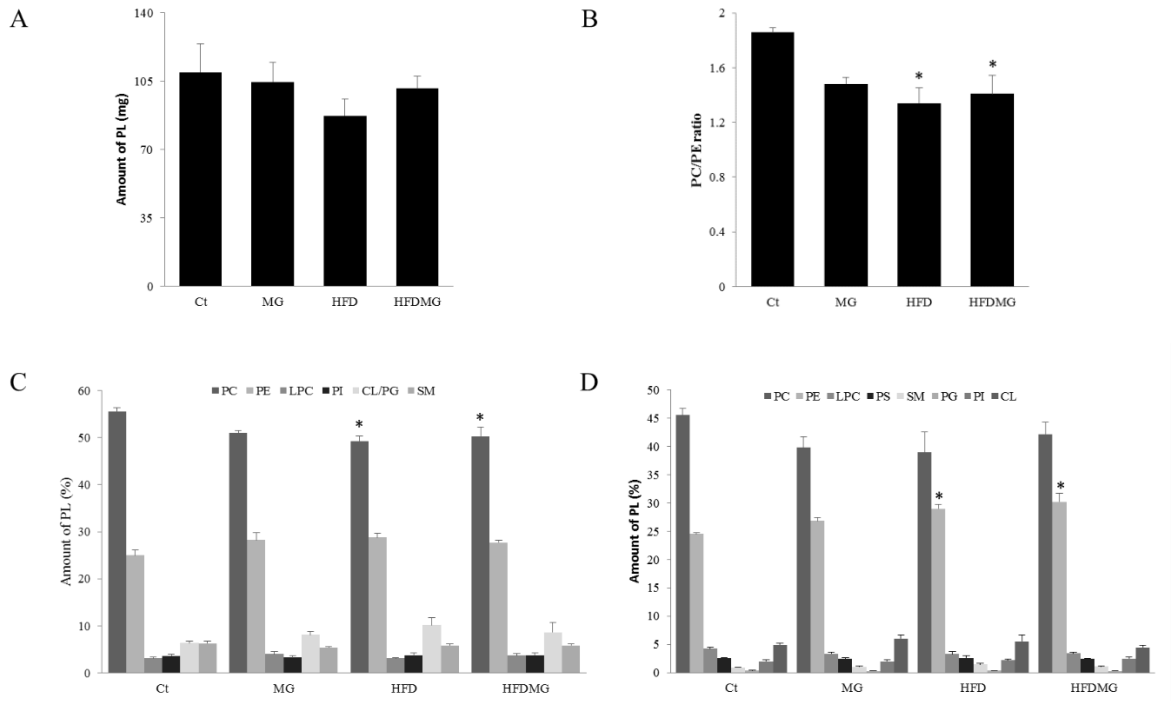

*Figure 21: Total amount of PL per gram of liver (A), PC/PE ratio (B), total amount of PL per class obtained by TLC (C) and HPLC-MS/MS (D). *different from Ct. 1 symbol p<0.05.*

HFD and HFDMG groups showed a decrease of PC levels by TLC and an increase of the total levels of PE in HPLC-MS/MS. The techniques have different sensitivity, however the values for all classes have the same trend. Ratio PC/PE performed by TLC or HPLC-MS/MS show a statistically significant decrease in fat diet administration groups (HFD and HFDMG). No differences were found in the other classes (Figure 21).

In the analysis by HPLC-MS/MS were identified and quantified the different species of PL classes and their constituent fatty acids (Table 7 and Table 8). All classes were identified in the negative mode and only PC, LPC and SM were identified as acetate (+58 m/z). The most abundant classes are PC-16:0/18:2 (m/z at 816), PC-16:0/20:4 (m/z at 840), PC-18:2/18:0 (m/z at 844), PC-20:4/18:0 (m/z at 868), PE-16:0/20:4 (m/z at 738), PE-18:2/18:2 (m/z at 738), PE-16:0/22:6 (m/z at 762), PE-18:2/20:4 (m/z at 762), PE-18:1/20:4 (m/z at 764), PE -18:0/20:4 (m/z at 766), LPC-16:0 (m/z at 554), LPC-18:0 (m/z at 582), PS-18:0/20:4 (m/z at 810), PS-18:0/22:6 (m/z at 834), SM-16:0

(m/z at 761), PG-16:0/18:1 (m/z at 747), PI-18:0/20:4 (m/z at 885), PI-18:1/22:6 (m/z at 907), CL-16:1/16:1/16:1/16:1 (m/z at 1343) and CL-18:2/18:2/18:2/18:2 (m/z at 1447).

PC plasmalogens identified have a tendency to diminish, although they have not a statistically significant difference (O-PC: m/z at 802, 830, 854 and 882). To following PE plamalogens, were also identified: O-PE: m/z at 700, 722, 728, 750, 752, 776 and 778, which only the O-PE-16:1/20:4 (m/z at 722) and O-PE-18:0/20:4 (m/z at 752) showed a statistically significant decrease in HFD and HFDMG groups (Table 7 and Figure 22B). In HFD group was observed a decreasing in PC-16:1/18:2 (m/z at 814), PC-16:1/20:4 (m/z at 838), PC-18:1/20:4 (m/z at 866) and PC-18:1/22:6 (m/z at 890). Regarding to PE, PE-18:1/20:4 (m/z at 764) decreased in both HFD and HFDMG groups and PE-18:0/20:4 (m/z at 766) increased only in HFD group (Figure 22A and B). PS and LPC were no statistically significant differences between groups, although it appears a tendency for LPC increasing their levels in HFDMG group. SM-18:0 (m/z at 789) increased in HFDMG group and SM-24:1 (m/z at 871) and SM-24:0 (m/z at 873) decreased in HFD group (Figure 22C). In HFD and HFDMG groups decreased PG-18:2/20:4 (m/z at 793) and PI-18:0/22:6 (m/z at 909). As for CL, there is a decrease of CL with m/z at 1313 in HFD and HFDMG groups and CL with m/z at 1471 only in HFDMG group (Figure 22D, E and F).

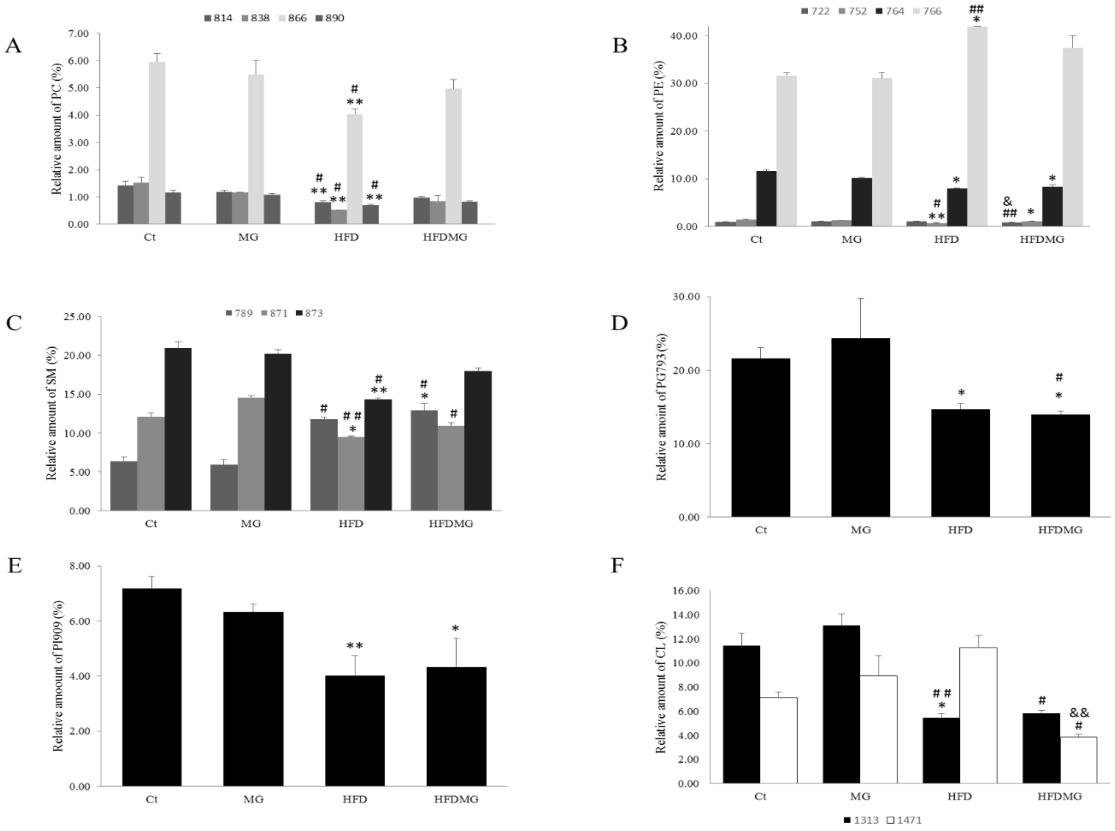

*Figure 22: Relative amount of PC, PE, SM, PI, PG and CL classes with statistically significance difference, by HPLC-MS/MS. *different from Ct. # different from MG. & different from HFD. 1 symbol p<0.05, 2 symbols p<0.01.*

*Table 7: Relative amount of different species of PC and PE, with respective fatty acid constitution and statistical p-value by HPLC-MS/MS. ** identified fatty acids in MS/MS. *** less abundant fatty acids.*

Class of PL	m/z	Species	Ct	MG	HFD	HFDMG	p-value
PC [M+CH3COO]-	790	16:0/16:1	0.96± 0.38	0.48± 0.05	0.44± 0.06	0.49± 0.05	-
	792	16:0/16:0	2.43± 0.32	2.39± 0.19	1.97± 0.13	2.08± 0.05	-
	802	O-16:0/18:0	3.60± 0.81	3.18± 0.63	2.59± 0.88	2.30± 0.43	-
	814	16:1/18:2	1.42± 0.16	1.19± 0.05	0.80± 0.05	0.97± 0.07	p<0.05
	816	16:0/18:2**	14.82± 0.89	16.45± 0.09	11.41± 0.56	12.36± 2.17	-
	830	O-18:0/18:2 O-18:1/18:1	2.10± 0.37	1.55± 0.11	1.99± 0.93	1.48± 0.15	-
	838	16:1/20:4	1.53± 0.20	1.17± 0.00	0.52± 0.00	0.85± 0.20	p<0.05
	840	16:0/20:4**	17.45± 0.40	18.06± 0.60	16.26± 1.60	15.01± 1.20	-
	844	18:2/18:0**	9.16± 0.31	9.16± 0.18	8.84± 0.87	9.79± 0.66	-
	854	O-18:0/20:4	4.81± 0.41	4.11± 0.57	6.66± 1.58	4.73± 0.63	-
	864	22:6/16:0**	7.87± 0.57	7.29± 0.27	5.96± 0.11	6.98± 0.58	-
	866	18:1/20:4**	5.96± 0.29	5.49± 0.50	4.04± 0.19	4.97± 0.34	p<0.05
	868	20:4/18:0	20.72± 1.66	22.37± 0.36	31.91± 2.62	30.74± 3.45	-
	882	O-18:0/22:4***	0.71± 0.11	0.63± 0.03	0.46± 0.07	0.52± 0.04	-
	888	18:2/22:6 20:4/20:4	1.02± 0.03	1.03± 0.06	0.89± 0.03	0.82± 0.07	-
	890	18:1/22:6**	1.16± 0.08	1.08± 0.05	0.70± 0.03	0.83± 0.03	p<0.05
	892	22:6/18:0**	4.27± 0.41	4.35± 0.05	4.56± 0.09	5.08± 0.58	-
PE [M+H]-	700	O-16:1/18:2	0.81± 0.12	0.57± 0.15	0.48± 0.02	0.80± 0.36	-
	722	O-16:1/20:4	0.94± 0.03	1.07± 0.01	1.00± 0.05	0.82± 0.05	p<0.05
	728	O-18:0/18:2 O-18:1/18:1	0.76± 0.10	0.66± 0.03	0.34± 0.03	0.42± 0.09	-
	738	16:0/20:4 18:2/18:2	11.27± 0.73	13.10± 0.19	10.90± 0.17	11.12± 0.85	-
	742	18:0/18:2** 18:1/18:1**	7.16± 0.58	8.52± 0.36	5.86± 0.46	7.62± 0.25	-
	750	O-18:1/20:4	1.31± 0.06	1.24± 0.14	2.02± 0.14	1.80± 0.24	-
	752	O-18:0/20:4	1.38± 0.04	1.26± 0.02	0.67± 0.03	0.98± 0.07	p<0.05
	762	16:0/22:6** 18:2/20:4**	19.06± 0.62	18.99± 0.66	17.01± 0.31	17.86± 0.96	-
	764	16:0/22:5*** 18:1/20:4**	11.56± 0.34	10.11± 0.17	7.91± 0.14	8.37± 0.33	p<0.05
	766	18:0/20:4**	31.59± 0.67	31.05± 1.15	41.94± 0.05	37.42± 2.59	p<0.05
	776	O-18:0/22:6	1.42± 0.43	0.69± 0.05	0.59± 0.05	0.85± 0.14	-
	778	O-18:0/22:5***	1.23± 0.43	0.86± 0.18	0.66± 0.06	0.54± 0.05	-
	788	18:1/22:6	1.81± 0.24	1.82± 0.06	1.13± 0.04	1.33± 0.25	-
	790	18:0/22:6**	9.71± 0.20	10.07± 0.36	9.49± 0.08	10.08± 0.18	-

*Table 8: Relative amount of different species of LPC, PS, SM, PG, PI and CL, with respective fatty acid constitution and statistical p-value, by HPLC-MS/MS.*carbons number/double bounds. ** identified fatty acids in MS/MS. *** less abundant fatty acids.*

Class of PL	m/z	Species	Ct	MG	HFD	HFDMG	p-value
LPC [M+CH3COO]-	554	16:0	13.92± 1.18	13.41± 0.65	11.58± 1.7	12.15± 1.0	-
	578	18:2	7.27± 0.21	6.87± 0.61	4.84± 0.2	6.22± 0.7	-
	580	18:1	6.25± 1.85	5.30± 0.66	4.86± 0.4	6.08± 1.0	-
	582	18:0**	59.05± 0.70	59.25± 3.09	66.86± 3.2	59.16± 1.9	-
	602	20:4	8.96± 0.79	10.01± 1.31	7.47± 1.0	10.74± 0.2	-
	624	22:5***	1.14± 0.06	1.48± 0.06	1.57± 0.2	1.68± 0.1	-
	626	22:6	3.41± 0.57	3.67± 0.20	2.84± 0.5	3.98± 0.3	-
PS [M+H]-	760	18:0/18:1**	11.70± 5.34	8.50± 1.00	7.84± 3.4	4.92± 1.7	-
	780	16:1/20:4**	7.62± 0.60	5.23± 0.72	3.26± 0.4	3.08± 0.4	-
	810	18:0/20:4**	48.83± 3.59	52.27± 1.49	58.80± 2.6	63.40± 2.4	-
	834	18:0/22:6**	31.85± 3.01	33.99± 1.49	30.09± 2.1	28.60± 2.3	-
SM [M+CH3COO]-	761	16:0	45.64± 1.64	46.85± 0.57	55.03± 0.49	46.79± 0.75	-
	789	18:0	6.38± 0.54	5.91± 0.64	11.82± 0.23	12.92± 0.83	p<0.05
	871	24:1	12.13± 0.45	14.55± 0.28	9.50± 0.12	10.94± 0.38	p<0.05
	873	24:0	20.94± 0.79	20.22± 0.51	14.36± 0.20	17.99± 0.42	p<0.05
PG [M+H]-	745	16:0/18:2	7.74± 1.2	7.93± 1.3	10.43± 0.3	8.87± 1.6	-
	747	16:0/18:1	55.63± 3.2	54.35± 4.4	58.41± 3.2	59.42± 5.7	-
	765	16:1/20:5***	14.99± 1.8	13.35± 1.7	16.45± 2.8	17.71± 4.2	-
	793	18:2/20:4	21.63± 1.4	24.37± 5.4	14.72± 0.7	14.00± 0.4	p<0.05
PI [M+H]-	831	16:1/18:2	1.94± 0.05	1.72± 0.42	1.90± 0.28	2.02± 0.48	-
	857	16:0/20:4 18:2/18:2	9.42± 0.48	8.02± 0.53	6.89± 0.23	6.59± 1.04	-
	861	18:0/18:2 18:1/18:1	7.50± 1.22	3.79± 0.91	2.60± 0.08	4.57± 1.05	-
	883	18:1/20:4	3.40± 0.18	3.14± 0.07	3.12± 0.44	1.85± 0.31	-
	885	18:0/20:4**	55.71± 7.82	59.57± 5.34	70.72± 6.65	73.66± 6.20	-
	907	18:1/22:6	14.86± 9.62	17.43± 6.09	10.77± 5.66	6.98± 3.32	-
	909	18:0/22:6	7.17± 0.45	6.33± 0.27	4.01± 0.72	4.33± 1.04	p<0.05
CL [M+H]-	1261	(C58:3)*	6.86± 1.14	5.71± 0.36	7.60± 1.32	5.70± 1.71	-
	1313	(C62:5)*	11.46± 1.03	13.14± 0.94	5.44± 0.39	5.82± 0.23	p<0.05
	1343	16:1/16:1/16:1/16:1	10.37± 0.35	8.49± 1.48	8.61± 2.02	12.07± 0.98	-
	1421	18:2/18:2/18:2/16:1	5.40± 1.00	5.21± 0.75	4.00± 0.45	5.45± 0.10	-
	1423	18:2/18:2/18:2/16:0	4.49± 0.32	4.66± 0.92	2.18± 0.75	3.80± 0.11	-
	1447	18:2/18:2/18:2/18:2**	21.59± 1.55	20.67± 0.86	28.67± 3.38	30.07± 1.97	-
	1471	(C74:10)*	7.13± 0.46	8.93± 1.69	11.28± 1.00	3.83± 0.26	p<0.05
	1473	(C74:9)*	9.41± 0.24	11.74± 1.65	11.57± 1.05	12.39± 1.12	-
	1523	(C78:12)*	7.38± 0.29	6.86± 0.35	5.96± 0.56	7.10± 0.47	-

4. Lipidemia and lipid Metabolism Regulation

NMR and lipidomic techniques revealed alterations in groups maintained with high-fat diet, but given the alterations in the saturation of fatty acids in HFDMG group, it is important to analyze the regulation of pathways involved in lipid metabolism and insulin signaling.

Plasma total cholesterol levels were increased in the HFD group, with a trend to increment in HFDMG group. TG levels didn't have differences between groups (Table 9).

*Table 9: Systemic levels of TG, total cholesterol and HDL cholesterol analyzed at Hospital and by commercial kit (TG). *different from Ct. # different from MG. 1 symbol p<0.05.*

Group	Ct	MG	HFD	HFDMG
Triglicerydes (mg/dl)	75.42± 5.52	69.33± 10.68	77.75± 5.37	62.29± 3.23
Total Cholesterol (mg/dl)	75.08 ± 4.62	72.33 ± 2.73	99.17± 9.44 *#	91.71 ± 8.80
HDL Cholesterol (mg/dl)	44.54± 2.73	45.75± 1.38	58.17± 4.71	55.71± 5.13

Regarding plasma FFA values, a significant increase was observed only in the HFDMG group. Consistently, plasma adiponectin levels were increased in the HFD group, but not in HFDMG (Figure 23).

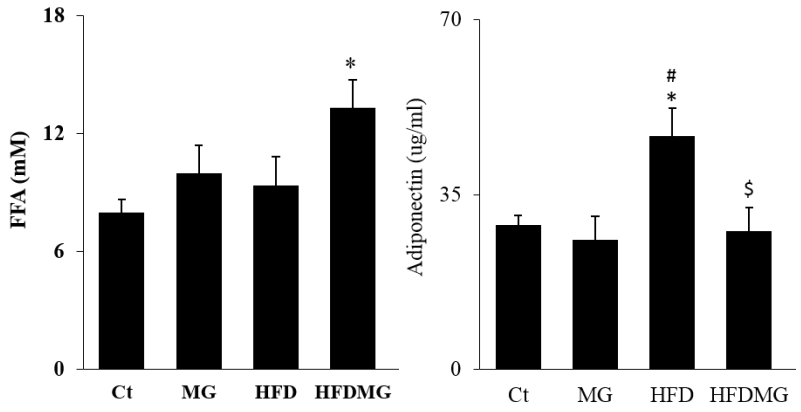

*Figure 23: FFA and adiponectin levels in plasma per group, analyzed by spectrophotometry and immunoassay kit, respectively. *different from Ct. # different from MG. $ different from HFD. 1 symbol p<0.05.*

Figure 24 shows values of total and phosphorylated levels of liver AMPK and although no significant differences are observed in the total and phosphorylated (active) forms of AMPK, the ratio between them decreased in HFD group, and especially in HFDMG.

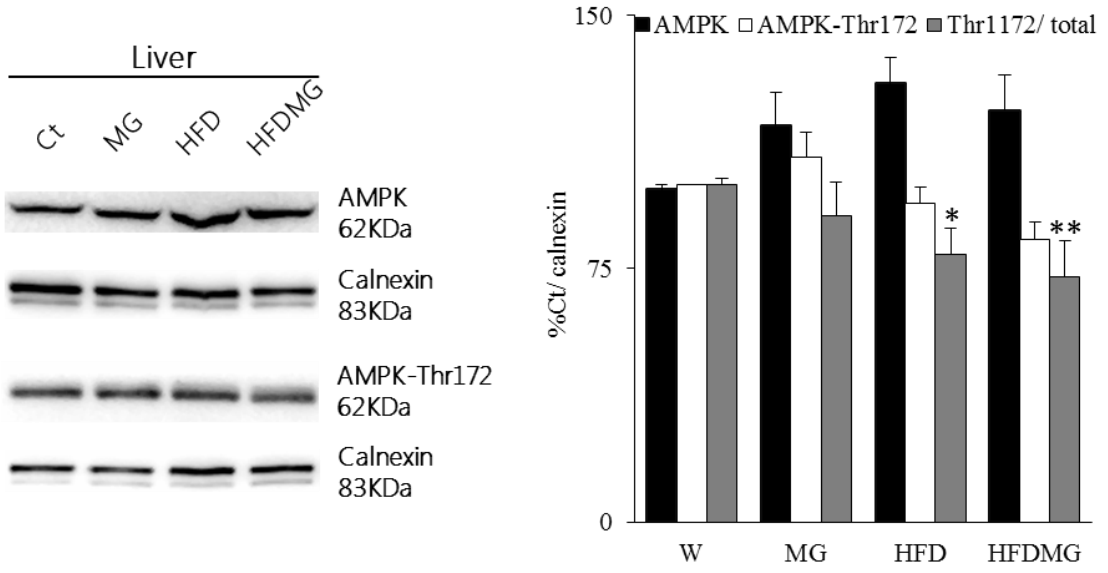

*Figure 24: Liver levels of total AMPK and Thr172-phosphorylated AMPK and ratio by western blotting. *different from Ct. 1 symbol p<0.05.*

ACC is phosphorylated (inactivated) by AMPK and, despite no differences were observed in the total amounts of the protein, the phosphorylated form (inactive) was increased in the HFDMG group and especially in HFD. Such alterations resulted in a significant increase of the ratio between the inactive and total forms in the HFD group, which was more modest in the HFDMG group (figure 25). (Figure 25).

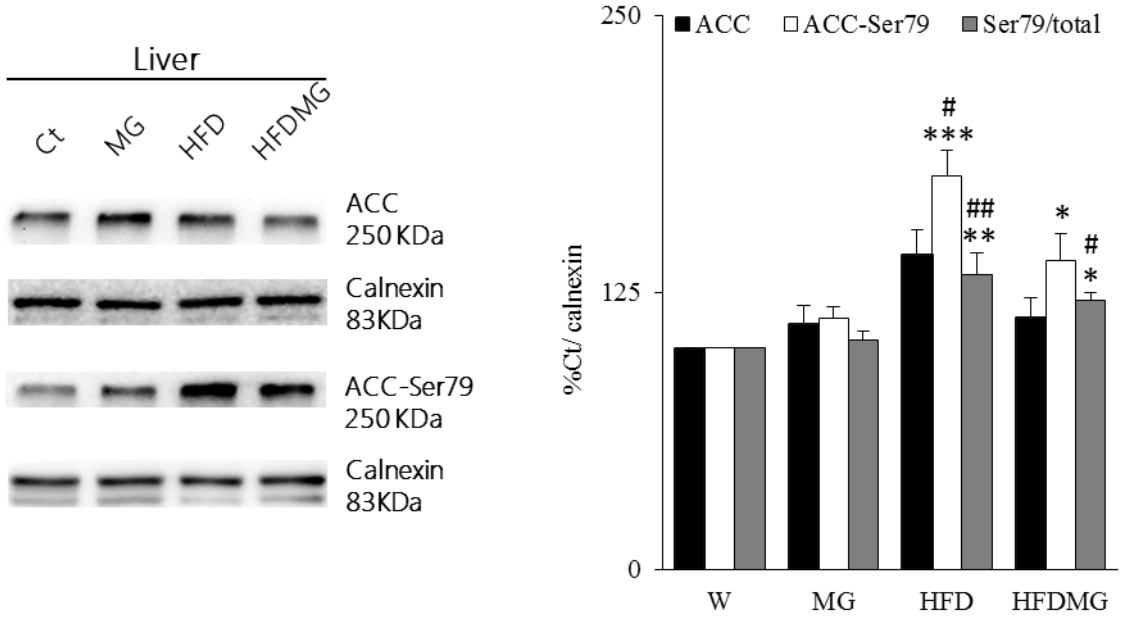

*Figure 25: Liver levels of total ACC and Ser79-phosphorylated ACC and ratio by western blotting. *different from Ct. # different from MG. 1 symbol p<0.05. 2 symbols p<0.01. 3 symbols p<0.001.*

5. Glycemia, HbA1c and glucose tolerance test

Regarding to plasma levels of glucose and glycated hemoglobin, these parameters showed no alterations, despite a trend to elevated glycated hemoglobin was found in HFDMG group (Figure 26).

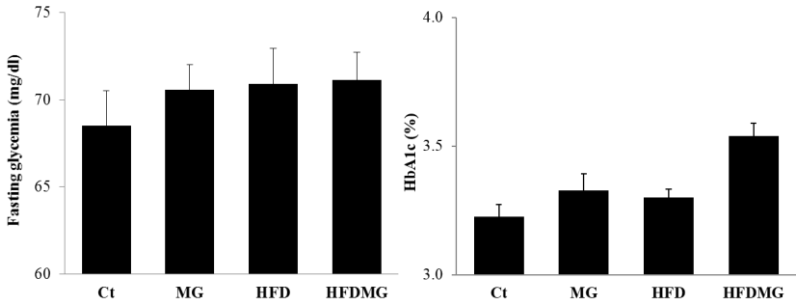

Figure 26: Plasma levels of fasting glycemia and hemoglobin glycated HbA1c, analyzed at Hospital and HbA1c analyzer.

The intraperitoneal glucose tolerance test was showed a reduced glucose tolerance in HFD group with higher area under the curve and glycemia at 2 hours, which is potentiated by the supplementation of MG (HFDMG) (Figure 27).

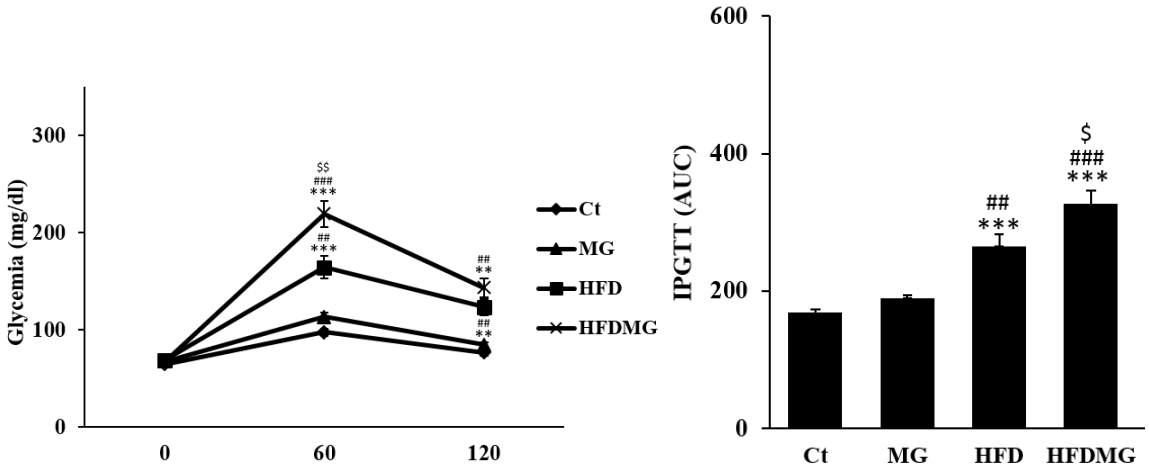

*Figure 27: Two hours (120 minutes) glycemia registration and area under curve of intraperitoneal glucose tolerance test (IPGTT). *different from Ct. # different from MG. $ different from HFD. 1 symbol p<0.05. 2 symbols p<0.01. 3 symbols p<0.001.*

6. Glucose metabolism regulation

In order to analyze the regulation of glucose metabolism, plasma insulin levels were evaluated, showing increased levels only in HFDMG group (Figure 28).

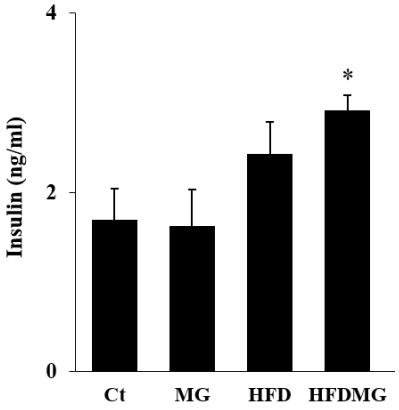

*Figure 28: Plasma levels of insulin by ELISA kit. *different from Ct. 1 symbol p<0.05.*

Accordingly, despite the total and phosphorylated (active form) levels of the insulin receptor showed no significant changes, the ratio presented a significant decrease in the HFD and HFDMG groups, being more evident in the last one (Figure 29).

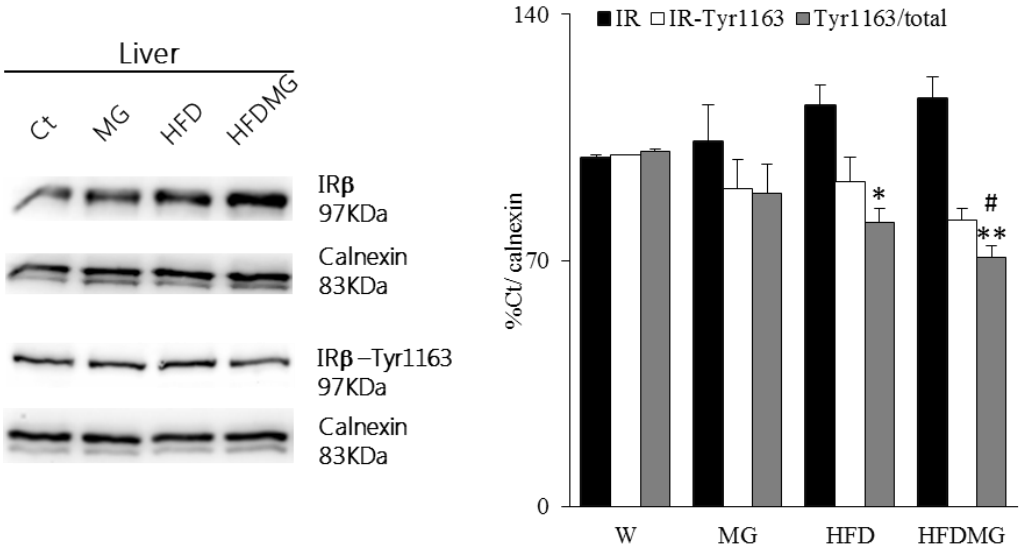

*Figure 29: Liver levels of Insulin Receptor (IR) and Tyr1163-phosphorylated IR and ratio, by western blotting. *different from Ct. # different from MG. 1 symbol p<0.05. 2 symbols p<0.01.*

Figure 30 presents the total levels of Akt and phosphorylated form (active), demonstrating a statistical reduction in levels of active Akt and ratio in the MG, HFD and HFDMG groups, especially in HFD and HFDMG groups.

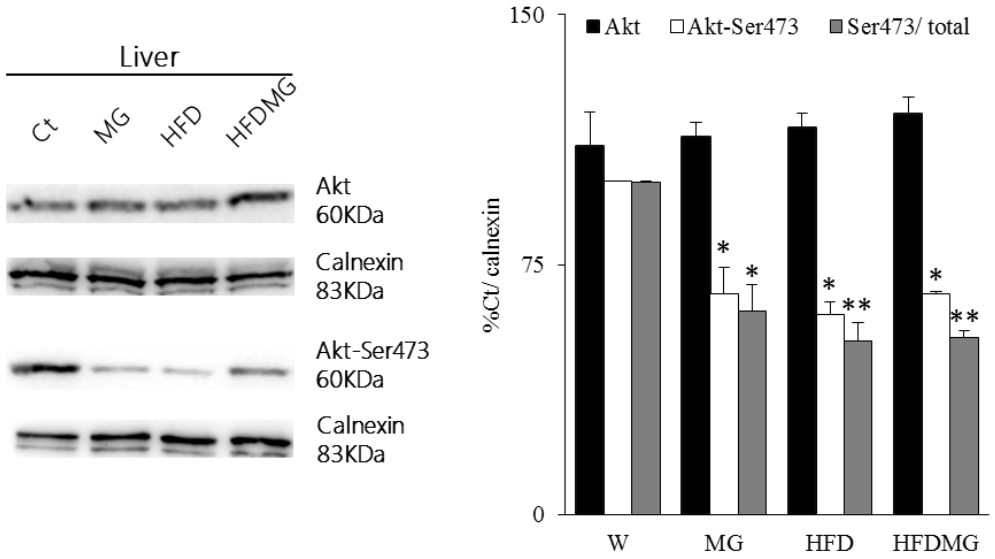

*Figure 30: Liver levels of Akt and Ser473-phosphorylated Akt and ratio by western blotting. *different from Ct. 1 symbol p<0.05.*

The GLUT2 levels were also determined, with a significant increase only in the HFD group, which is consistent with a compensatory mechanism for glucose uptake. This was not observed in HFDMG group (Figure 31).

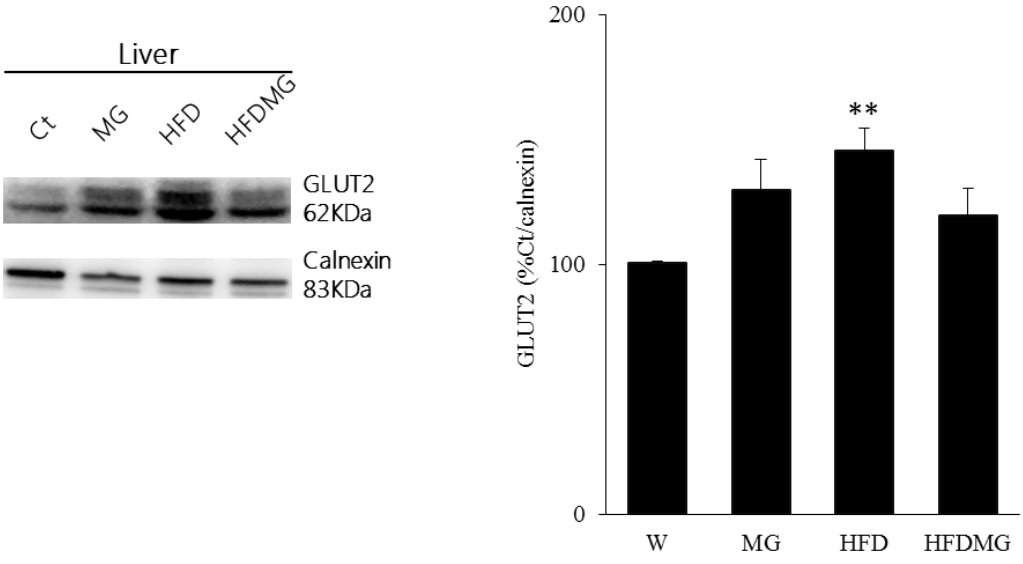

*Figure 31: Liver levels of GLUT2 by western blotting. *different from Ct. # different from MG. 2 symbols p<0.01.*

CHAPTER 5

DISCUSSION

Discussion

This work was designed to assess the involvement of glycation induced by methylglyoxal in the impairment of hepatic lipid metabolism, given that lipotoxicity is a known mechanism causing inflammation and insulin resistance. Such mechanisms may be involved in the progression of obesity and pre-diabetes to type 2 diabetes.

Previous studies confirmed that the glycation process is implicated in microvascular complications of type 2 of diabetes mellitus, independent of obesity and that plasma levels of methylglyoxal are increased in diabetic patients and animal models (22–24). As well, our group recently showed that oral MG administration may have functional consequences in insulin-sensitive tissue, namely the adipose tissue and the muscle (22,26–28)(unpublished data). Knowing this, it is expectable that MG-induced glycation may have consequence for the hepatic lipid metabolism in obesity.

High-fat diet-induced mechanisms of lipid and glucose storage

It was pertinent to evaluate the characteristics of fatty liver developed in an obese model in the presence of glycation, which is characteristic of diabetes and pre-diabetes states, and analyze the pathophysiological differences between them, given that obese patients have a higher risk for developing diabetes, but not all obese patients develop the disease nor NASH (3,30).

Under normal feeding conditions, the intake of carbohydrates and fats is compensated by insulin levels, allowing the liver to increase glycolysis and glycogenesis, to reduce the plasma glucose and produce ATP. In the adipocyte, the hormone-sensitive lipase (47) is inhibited to prevent lipolysis and stimulate lipid storage by the activation of lipoprotein lipase (48); this mechanism removes blood fats and store them in adipocytes for when energy will be required.

In high-fat diet-fed condition, insulin will respond to this increase to metabolize the post-prandial glucose with glycolysis and glycogen synthesis and adipocytes will store the fats ingested. The reasons that limit adipocyte's ability to store fat are currently under investigation, but are believed to be related to hypoxia and inflammation. Therefore, if adipose tissue reaches its limit, there is an increased lipolysis, increased plasma FFA levels and compensation by the liver to reduce this increment. Insulin action deviate FFA for the de novo synthesis of PL, glycerolipids and cholesterol esters, in this order, releasing them in the form of VLDL or store them as lipid droplets (in exacerbated cases, such as obesity). The liver compensates FFA levels during fasting phase, with β-oxidation or cholesterol synthesis if it does not require energy supply (10).

Hepatic Lipotoxicity

HFD and HFDMG groups consumed the same amount of high-fat diet, which is rich in MUFA (18:1) and SFA (16:0 and 18:0). At the end of the treatment there was a substantial increase in body weight only in HFD group. In HFDMG group, the weight increase was not so pronounced, suggesting an interference of methylglyoxal in the normal lipid storage and metabolism. According to studies conducted by our group at the Laboratory of Physiology (IBILI), methylglyoxal have effects on the microvasculature of the adipose tissue and thereby create hypoxic regions leading to dysmetabolism. Thus, impaired adipose tissue expandability may explain the lower body weight in HFDMG group (26). However, given the importance of the adipose tissue in properly storing dietary lipids, one may believe that profound changes in lipid metabolism will occur.

Liver weight was similar in all groups, thus the ratio of liver weight/body weight decreased in HFD and HFDMG groups. However, it was possible to observe fat deposition in the liver of HFD and HFDMG groups in the macroscopic analysis; this is characteristic of hepatic steatosis, although the liver function tests still remain normal and it is necessary a histological confirmation.

It is expected that adipose tissue dysmetabolism causes lipolysis, with FFA release to the circulation, inducing hepatic accumulation (3,10,31,36). HFD group shows normal plasma FFA, meaning that fat is being accumulated in adipose tissue, what is consistent with increased fat mass in this group (data not shown). Alternatively, liver may accumulate triglycerides in lipid droplets or use fatty acids to the cholesterol synthesis, which is consistent to increased serum cholesterol levels is this group, despite the normal cholesterol levels of the diet .

In order to evaluate lipid accumulation in liver, 1H NMR and lipidomic approaches were performed, as they emerged as powerful tools for the profiling and characterization of lipids *ex vivo* (biopsies) and *in vivo*. Higher amounts of fat were observed in the HFD and HFDMG groups, with no differences in the total amount of phospholipid per gram of liver. Thus, despite the change in the amount and species of fatty acids caused by the diet, the total amount PL was kept constant (49). Importantly, we observed changes in the levels of specific species of PLs, which physiological significant should be addressed in the future. Of significance is the fact that cardiolipins, present in the mitochondria membranes, were decreased in the HFDMG group, suggesting a higher level of mitochondria dysfunction.

Regarding fatty acid species, total MUFA were increased in the HFD group while the PUFA decreased in both groups (HFD and HFDMG) (3), because the diet has a high content of SFA and MUFA. Increased MUFA levels in the HFD group result from the abundant amount of oleic acid (18:1) in the diet, but also from the shift from saturated towards unsaturated fatty acyl chains

catalyzed the enzyme SCD1. In HFDMG group, such mechanisms appear to be impaired. Although they ingest the same amount of saturated fatty acids and MUFA, their liver content are different than in HFD rats. This may result from changed SCD1 activity in this group, increased oxidative modification or increased β-oxidation of MUFA. Although increased β-oxidation could be consistent with the hyperinsulinemia and insulin resistance observed in this group, AMPK levels were diminished. Furthermore, high levels of FA-CoA decrease ACC, deviating fatty acids to oxidation. In order to address this, PPARα levels should be determined, as it controls β-oxidation. In obesity, fats are deviated to the synthesis of glycerolipids, increasing lipid droplets; these lipid droplets increase interaction with microsomal lipase and it increases the FA-CoA formation, which in turn will inhibit ACC. However, HFDMG group showed less inactive form (phosphorylated) of ACC than HFD group, which is consistent to increased SCD1 activity in this group. Moreover, adiponectin levels are increased in HFD group, stimulating oxidation of fatty acids, which is not observed in HFDMG group (33,34,50). Interestingly, TGs have higher affinity to esterify MUFA than SFA, but this is not observed in HFDMG group. Such observations suggest that instead of increased β-oxidation, decreased MUFA levels in HFDMG group may derive from increased oxidative modification in inappropriate SCD1 activity (future work).

Regarding saturated lipids, they have more affinity to be incorporated in DAG. Although DAG quantification in liver should be performed in the future, magnetic resonance imaging suggested the existence of increased levels. Consistent with increase MUFA and possibly with increased SCD1 activity, HFD group had equal (16:0) or decreased (18:0) esterified SFA than controls. In normal conditions, insulin stimulates SCD1 gene expression via-SREBP1, reducing SFA and increasing MUFA to deviate them for synthesis of PL, TG and cholesterol esters or oxidation (16). HFDMG group did not show decreased SFA and increased MUFA esterification, suggesting increased DAG formation (15,51).

TG levels have a trend to increase in HFD group, with a large deviation in the HFDMG group, turning necessary to increase the samples number. However, according with the literature, hepatic TG are increased in obesity patients, accumulated in lipid droplets, but in diabetic patients, hepatic TG levels could be diminished, possible by inhibition of esterification, depending of insulin function, oxidative stress and pathology progression (3,52,53). Previous studies from QOPNA, University of Aveiro, using diabetic rats reveal the same alterations in liver associated to diabetic rat model (54).

The role of phospholipis in oxidative stress and inflammation

Esterified linoleic acid (18:2) did not change between groups. This fatty acid is essential for the formation of the PUFAs arachidonic acid (20:4) and docosahexaenoic acid (22:6), which are decreased in esterified lipids in high-fat diet-fed groups (3). The type 3 omega fatty acid (docosahexaenoic acid, 22:6) is a more effective activator of PPAR-α signaling than the type 6 omega fatty acid (arachidonic acid; 20:4). However, the reduction of esterification of both may denote an increase of their free levels, which could increases PPAR-α activation and suppress SREBP1. This would induce fatty acid oxidation and VLDL secretion and reduces cholesterol and fatty acid synthesis, in the end decreasing hepatic lipid accumulation (52). On the other hand, increased availability of arachidonic acid seems to result in enhanced production of proinflammatory molecules in liver, by the reaction with cycloxygenase and lipoxygenase and overproduction of prostaglandins and leukotrienes; this contributes to development of the inflammation, activation of Kupffer cells and NASH (52,55,56).

Plasmalogen PE are free radical scavengers, which are decreased in metabolic syndrome and diabetes, suggesting an elevation of hepatic oxidative stress and impairment of the antioxidant capacity (57). We observed decreased plasmalogen PE in HFD rat, but mostly in HFDMG. This is consistent with increased SM-18:0 levels in HFDMG, which was previously associated with impaired liver function (58). The decreased levels of PG and PI founded in HFD and HFDMG groups are associated to the decreased levels of esterified arachidonic and docosahexaenoic acids. Similarly, CL are present in the mitochondrial membrane, being sensitive to reactive species of oxygen due to high content of unsaturated fatty acids, but may be also involved in the protection against ROS. We observed that HFDMG group has further decreased levels of the CL 1313 and 1471, suggesting an increased ROS production (59).

Regarding PL classes, the PC/PE ratio decreased in the HFD and HFDMG groups, which means PC are decreasing, by inactivation of PE N-methyltransferase (Pemt), and PE are increasing, impairing membrane integrity and starting a process of hepatic dysfunction (3,60). A study from Chitraju et al. (2012) used high-fat diet-fed rats and another from Zhaoyu et al. (2006) induced steatohepatitis in Pemt-/- mice, and they showed a decreased PC/PE ratio too, considering an interesting marker of inflammation. Similarly, several studies have shown that diabetic models have decreased levels of this enzyme (61,62). Pmet activity may be regulated by insulin and glucagon, although the mechanisms are currently unknown (63–65).

Insulin resistance

Magnetic resonance imaging suggested increased DAG levels in HFDMG group, due to a decrease in the percentage of esterification. DAG is known to be a strong inducer of insulin resistance and lipotoxicity (10,32,36). The calculation of glycerol esterification and FA/glycerol ratio suggest the levels of DAG and NEFA, respectively. The use of this formula is based on the fact that 1,2-DAG and 2,3-DAG are more abundant in the cell(>70%) (66) as they are obtained from glycerolipid synthesis (1,3-DAG is produced only during TG hydrolysis) (63). FA/glycerol ratio was bigger than 1, which means that there are more FA than glycerol molecules and thus NEFA. So, crossing the results from ^{1}H NMR and lipidomic, the amount of esterified fatty acids is increased only in HFD group, while HFDMG group appears to have more NEFA. Therefore, such changes in the HFDMG group will have a strong influence on liver lipid oxidation and insulin signaling. This group also has glucose intolerance at 2 hours, hyperinsulinemia, hypoadiponectinemia and increased plasma FFA levels (3,10,22,23).

Adiponectin secretion and circulating levels were shown to be decreased in diabetic patients (24), reducing lipid oxidation capability and contributing to NAFLD and hepatic and peripheral insulin resistance (3,24,32). Active/total AMPK ratio was decreased in HFD and HFDMG groups, but this was more evident in HFDMG group, further supporting the idea of impaired lipid β -oxidation. This may derive from hypoadiponectinemia or inactivation of Akt.

A decrease of the active form of the insulin receptor and consequently less active Akt were observed in the HFD group and further in the HFDMG group, indicating that the liver needs to increase the overall levels of insulin receptor to achieve its activation. Insulin promotes the synthesis of glycerolipids (TG, PL), retaining them in lipid droplets or releasing them with VLDL, despite high insulin levels diminish the production of lipoproteins, independently of FFA levels (3,67). Thus, insulin resistance predisposes to increased acetyl-CoA accumulation by β-oxidation, causing mitochondrial dysfunction. This will cause the activation of the microsomal lipid peroxidases-mediated PUFA peroxidation (3,67). GLUT2 levels were elevated in HFD group, what is expected, given that its gene expression is stimulated by elevated levels of MUFA, independent of hyperglycemia. GLUT2 levels are also upregulated in insulin-resistance and when gluconeogenesis stimulation. In HFDMG group, GLUT2 levels are not different from control group, what is consistent with lower 18:1 levels than HFD rats and decreased activity of the insulin receptor pathway (68).

Thus, our results show that glycation further decreases the activity of the insulin-Akt pathway and hyperinsulinemia in obesity. Such events may apparently result from impaired lipid

metabolism, lipotoxicity and oxidative stress, deviating the metabolic process, with inhibition of glycolysis and glycogen synthesis and overstimulating lipid oxidation.

NAFLD and NASH

It is important to distinguish liver steatosis in obese and type 2 diabetic patients. Although the diet in both pathologies is based on the same saturated fats, the body will respond in different ways. It can be assumed that obesity can be inducing an early stage of diabetes, but the patient may never develop chronic hyperglycemia and microvascular complications associated to glycation. Therefore, it should be recalled that an obese have an increase in adipocytes size and when it reaches its storage limit, the liver compensate the adipocyte failure, preventing early metabolic dysfunction.

Thus, obese patients may have hepatic steatosis and lipotoxicity associated with high saturated fat intake, but not yet systemic dysmetabolism, compensating elevated fatty acids with glycerolipids and cholesterol synthesis.

On the other hand, in diabetic patients, insulin resistance comes to disrupt hepatic glucose and lipid clearing, inducing systemic dysmetabolism and dysregulation of liver glucose and lipid metabolism, which may contribute to the progression of NAFLD to NASH. Moreover, the chronicity of the disease and oxidative stress damage in the liver, increasing the inflammatory process, leads to NASHS, this pathology needs a careful observation by health practitioner due to high risk progression to cirrhosis, liver failure or even hepatocellular carcinoma (52,53) (see Figure 32).

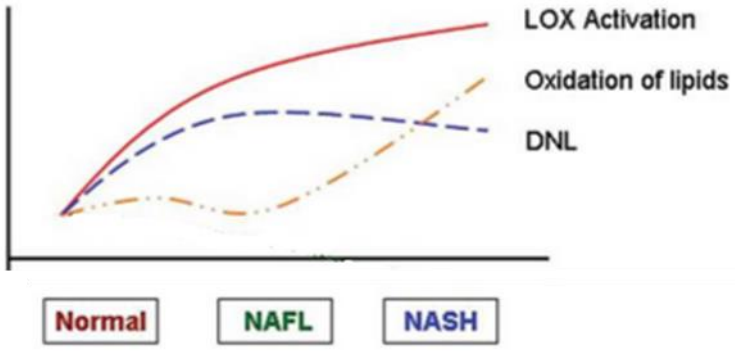

Figure 32: Adapted proposed model of lipotoxicity progression(53). *(LOX: lipoxygenase. DNL: De novo lipogenesis. NAFL: Non-alcoholic Fatty Liver. NASH: Non-alcoholic Steatohepatitis*

Integration of ^{1}HNMR with lipidomic approaches

^{1}H NMR and lipidomic approaches use has been increasing for the detection of lipid alterations in any tissue or body fluid due to its high sensitivity for detection of lipid species, therefore contributing to an improvement in lipidology and the analysis the beneficial and detrimental changes which can appear in specific diets and pathologies.

However, the techniques do not exhibit the same results and they are both necessary in order to obtain the largest possible information. Their use is however limited to the fact that in vivo organ analysis depends of biopsies, which is an invasive procedure difficult to implement in a large scale. 1H NMR allows a non-invasive determination of the amount of total fat, SFA, unsaturated fatty acids, MUFA and PUFA in vivo. If the sufficient field force is applied, it allows getting other parameters as the percentage of esterification of glycerol and the ratio FFA/glycerol, which estimate the amount of DAG and NEFA, respectively. However, given the different vibration of the lipids incorporated in a bilayer, this technique only allows the quantification of non-phospholipid lipids. In the other hand, lipidomics allow analyzing the total amount of PL, esterified fatty acids, including in the PL, and identify and quantify the species of fatty acids in each lipid classes; it is also possible to evaluate TG and DAG using mass spectrometry techniques, but the protocol still needs to be optimized. The disadvantage of the type of technique is the lack of sensitivity for non-esterified lipid species.

AGE and NAFLD/NASH crossover

There is not much information about the direct effect of glycation in NAFLD. Obese patients are also able to produce Amadori product through the intrahepatic oxidation of fatty acids consequent to lipid peroxidation, and independent of hyperglycemia-induced AGE formation. This event may explain the increased risk of NAFLD progression in obese patients without diabetes and thus to diabetes development itself. However, the levels of lipid-derived glycation products are small and they are only effective when there already lipotoxicity-induced liver changes, since the exogenous AGE without obesity have greater difficulty to induce NAFLD (69).

Some studies indicate that the formation of AGE will interact with receptors in hepatocytes (RAGE). RAGEs of the hepatocytes and stromal hepatic stellate cells (HSC) bind to AGEs, inducing oxidative stress, HSC proliferation and fibrosis, by NF-κB and JNK activation (70). JNK pathway inhibit IRS1, inducing insulin resistance, proinflammatory activation and lipotoxicity (71,72). More, it was observed that dietary AGE may cause liver inflammation in the absence of hepatic steatosis

(73). Another study shows a relation between AGE-induced oxidative stress with other liver pathologies, such as non-ischemic, ischemic injury and hepatocellular carcinoma (48).

A study with diagnosed hepatic steatosis, NAFLD and NASH patients revealed diminished plasma levels of soluble RAGE, but only in the last phase of the disease, indicating these receptors as a protective label to prevent the binding of AGE into tissues (74). On the other hand, glyceraldehyde-derived AGE is a plasmatic toxic AGE (TAGE) and it was recently demonstrated its effect in angiopathy from diabetes patients; it could be a novel biomarker for NASH due to the high levels in the end of progressive NAFLD (75). Such studies are in accordance with our data, showing that MG impairs lipid esterification, with increased saturation, having functional consequences in insulin signaling.

CHAPTER 6

FUTURE WORK

Future Work

At the present, the project continues with the analysis of inflammatory parameters associated to obesity, diabetes and NAFLD/NASH. It began with the labeling by western blotting of cells of the hepatic reticuloendothelial system (macrophages), Kupffer Cells, which are phenotypically positive for F4/80 and, according to the literature, they accumulate mainly in NAFLD and diabetes condition (Figure 33) (29,76).

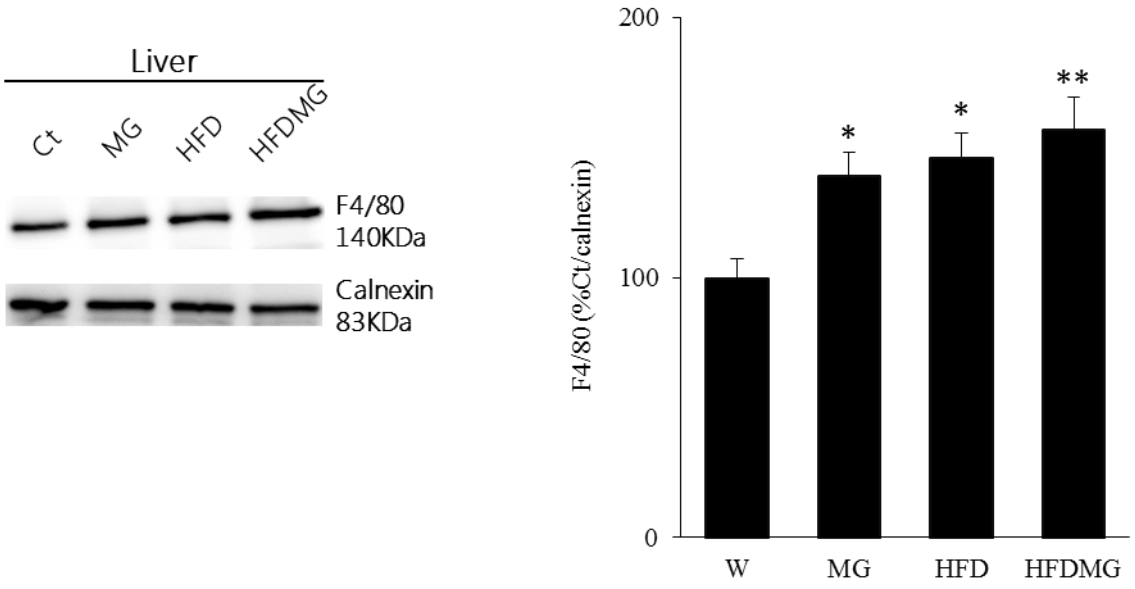

*Figure 33: Levels of liver macrophage marker F4/80. *different from Ct. 1 symbol p<0.05. 2 symbols p<0.01.*

Moreover, histological analysis is being performed at the Centro Hospitalar Universitário de Coimbra for further analysis of the presence of microscopic fat and inflammatory infiltration.

It is also necessary to increase the number of liver samples for lipidomic analysis, as well as determining the levels of total DAG and key enzymes involved in lipid metabolism such as SCD1. After finishing these processes, all relevant results will be published.

CHAPTER 7

CONCLUSION

Conclusion

To conclude, given the cause/consequence relationship between fatty liver disease and insulin resistance, this study aimed to evaluate the effects of glycation in lipotoxicity and thus the development of insulin resistance, contributing to this liver vicious cycle.

In high-fat diet-fed rats with methylglyoxal administration, the formation of AGE triggered a change in peripheral lipid metabolism, caused by the adipose tissue dysfunction and consequent increased plasma FFA levels. This increased FFA flux to the liver is also associated with increased markers of mitochondria oxidative damage. Mitochondrion dysfunction increases ROS, deflecting the process to the synthesis of TG and DAG (3,10). In turn, lipid species like DAG cause insulin resistance, what was observed in HFDMG rats. Thus, insulin resistance deregulates fatty acid oxidation and glycerolipids synthesis, perpetuating the vicious cycle that leads to NAFLD progression.

Thus, the deregulation of fat accumulation in liver as lipid droplets by MG-induced glycation contributes to hepatic lipotoxicity and insulin resistance. The evolution of such changes leads to the onset of NAFLD and NASH, characterized by a severe inflammatory process that can ultimately induce liver failure.

CHAPTER 7

BIBLIOGRAPHY

Bibliography

1. Systemic Veins. Structure of the Veins. Functions of the Veins [Internet]. [cited 2015 Jun 2]. Available from: http://encyclopedia.lubopitko-bg.com/Systemic_Veins.html

2. Boron WF, Boulpaep EL. Medical Physiology. 2008.

3. Tessari P, Coracina a, Cosma a, Tiengo a. Hepatic lipid metabolism and non-alcoholic fatty liver disease. Nutr Metab Cardiovasc Dis. Elsevier Ltd; 2009 May;19(4):291–302.

4. Huang W, Metlakunta A, Dedousis N, Zhang P, Sipula I, Dube JJ, et al. Depletion of liver Kupffer cells prevents the development of diet-induced hepatic steatosis and insulin resistance. Diabetes. 2010 Feb;59(2):347–57.

5. Kien CL, Heitlinger LA, Li BU, Murray RD. Digestion, absorption, and fermentation of carbohydrates. Semin Perinatol. 1989 Apr;13(2):78–87.

6. Fardilha M, Da Cruz e Silva OAB. O Essencial em... Sinalização Celular. 1ª ed. Edições Afrontamento; 2012.

7. Berridge MJ. Cell Signalling Biology. Portland P. 2012.

8. Berg JM, Tymoczko JL, Stryer L. Biochemistry. 5th ed. W H Freeman; 2002.

9. Lipid Metabolism [Internet]. [cited 2015 Jun 2]. Available from: https://lookfordiagnosis.com/mesh_info.php?term=lipid+metabolism&lang=1

10. Nguyen P, Leray V, Diez M, Serisier S, Le Bloc'h J, Siliart B, et al. Liver lipid metabolism. J Anim Physiol Anim Nutr (Berl). 2008 Jun;92(3):272–83.

11. King MW. Integrative Medical Biochemistry: Examination and Board Review. 1st ed. McGraw-Hill Professional Publishing; 2014.

12. Quintas A, Freire AP, Halpern MJ. Bioquimica - organização molecular da vida. 1st ed. LIDEL; 2008.

13. Sonntag AG, Dalle Pezze P, Shanley DP, Thedieck K. A modelling-experimental approach reveals insulin receptor substrate (IRS)-dependent regulation of adenosine monosphosphate-dependent kinase (AMPK) by insulin. FEBS J. 2012 Sep;279(18):3314–28.

14. Gray S, Kim JK. New insights into insulin resistance in the diabetic heart. Trends Endocrinol Metab. 2011 Oct;22(10):394–403.

15. Paton CM, Ntambi JM. Biochemical and physiological function of stearoyl-CoA desaturase. Am J Physiol Endocrinol Metab. 2009 Jul 1;297(1):E28–37.

16. Igal RA. Stearoyl-CoA desaturase-1: a novel key player in the mechanisms of cell proliferation, programmed cell death and transformation to cancer. Carcinogenesis. 2010 Sep;31(9):1509–15.

17. Vidal-alabró A, Méndez-lucas A, Semakova J, Gómez-valadés AG, Perales JC. Liver Glucokinase and Lipid Metabolism. Mitochondrion.

18. Schroepfer GJ. Oxysterols: modulators of cholesterol metabolism and other processes. Physiol Rev. 2000 Jan;80(1):361–554.

19. Baron AD, Brechtel-Hook G, Johnson A, Cronin J, Leaming R, Steinberg HO. Effect of perfusion rate on the time course of insulin-mediated skeletal muscle glucose uptake. Am J Physiol. 1996 Dec;271(6 Pt 1):E1067–72.

20. Bechmann LP, Hannivoort RA, Gerken G, Hotamisligil GS, Trauner M, Canbay A. The interaction of hepatic lipid and glucose metabolism in liver diseases. J Hepatol. 2012 Apr;56(4):952–64.

21. Nagan N, Zoeller RA. Plasmalogens: biosynthesis and functions. Prog Lipid Res. 2001 May;40(3):199–229.

22. Negre-Salvayre A, Salvayre R, Augé N, Pamplona R, Portero-Otín M. Hyperglycemia and glycation in diabetic complications. Antioxid Redox Signal. 2009;11:3071–109.

23. Brownlee M. The Pathobiology of Diabetic Complications: A Unifying Mechanism. Diabetes. 2005;54:1615–25.

24. Maury E, Brichard SM. Adipokine dysregulation, adipose tissue inflammation and metabolic syndrome. Mol Cell Endocrinol. 2010 Jan 15;314(1):1–16.

25. Matafome P, Sena C, Seiça R. Methylglyoxal, obesity, and diabetes. Endocrine. 2013 Jun;43(3):472–84.

26. Matafome P, Santos-Silva D, Crisóstomo J, Rodrigues T, Rodrigues L, Sena CM, et al. Methylglyoxal causes structural and functional alterations in adipose tissue independently of obesity. Arch Physiol Biochem. 2012 May;118(2):58–68.

27. Rodrigues T, Matafome P, Seic R. A vascular piece in the puzzle of adipose tissue dysfunction : mechanisms and consequences. 2013;3455:1–11.

28. Sena CM, Matafome P, Crisóstomo J, Rodrigues L, Fernandes R, Pereira P, et al. Methylglyoxal promotes oxidative stress and endotelial dysfunction. Pharmacol Res. 2012;

29. Schreuder TCM a, Verwer BJ, van Nieuwkerk CMJ, Mulder CJJ. Nonalcoholic fatty liver disease: an overview of current insights in pathogenesis, diagnosis and treatment. World J Gastroenterol. 2008 Apr 28;14(16):2474–86.

30. Gaggini M, Morelli M, Buzzigoli E, DeFronzo R a, Bugianesi E, Gastaldelli A. Non-alcoholic fatty liver disease (NAFLD) and its connection with insulin resistance, dyslipidemia, atherosclerosis and coronary heart disease. Nutrients. 2013 May;5(5):1544–60.

31. Bugianesi E, McCullough AJ, Marchesini G. Insulin resistance: a metabolic pathway to chronic liver disease. Hepatology. 2005 Nov;42(5):987–1000.

32. Ye J. Mechanisms of insulin resistance in obesity. Front Med. 2013 Mar;7(1):14–24.

33. Xu A, Wang Y, Keshaw H, Xu LY, Lam KSL, Cooper GJS. The fat-derived hormone adiponectin alleviates alcoholic and nonalcoholic fatty liver diseases in mice. J Clin Invest. 2003 Jul;112(1):91–100.

34. Kadowaki T, Yamauchi T. Adiponectin and adiponectin receptors. Endocr Rev. 2005 May;26(3):439–51.

35. Bugianesi E. Review article: steatosis, the metabolic syndrome and cancer. Aliment Pharmacol Ther. 2005 Nov;22 Suppl 2(May):40–3.

36. Neuschwander-Tetri B a. Hepatic lipotoxicity and the pathogenesis of nonalcoholic steatohepatitis: the central role of nontriglyceride fatty acid metabolites. Hepatology. 2010 Aug;52(2):774–88.

37. Rodrigues T, Matafome P, Seiça R. Methylglyoxal further impairs adipose tissue metabolism after partial decrease of blood supply. Arch Physiol Biochem. 2013 Dec;119(5):209–18.

38. Aued-Pimentel S, Lago JHG, Chaves MH, Kumagai EE. Evaluation of a methylation procedure to determine cyclopropenoids fatty acids from Sterculia striata St. Hil. Et Nauds seed oil. J Chromatogr A. 2004 Oct 29;1054(1-2):235–9.

39. Wang Y, Bollard ME, Keun H, Antti H, Beckonert O, Ebbels TM, et al. Spectral editing and pattern recognition methods applied to high-resolution magic-angle spinning 1 H nuclear magnetic resonance spectroscopy of liver tissues. Anal Biochem. 2003;323:26–32.

40. Folch J, Lees M, Sloane Stanley GH. A simple method for the isolation and purification of total lipides from animal tissues. J Biol Chem. 1957 May;226(1):497–509.

41. Feng J, Chen Y, Pu J, Yang X, Zhang C, Zhu S, et al. An improved malachite green assay of phosphate: mechanism and application. Anal Biochem. 2011 Feb 1;409(1):144–9.

42. Leray C, Pelletier X, Hemmendinger S, Cazenave J-P. Thin-layer chromatography of human platelet phospholipids with fatty acid analysis. J Chromatogr B Biomed Sci Appl. 1987 Jan;420:411–6.

43. Pulfer M, Murphy RC. Electrospray mass spectrometry of phospholipids. Mass Spectrom Rev. Jan;22(5):332–64.

44. NIH National Institute of General Medical Sciences, Dennis EA. LIPID Metabolites and Pathways Strategy (MAPS) [Internet]. 2003. Available from: http://www.lipidmaps.org

45. Ye Q, Friedrich C, Fuchs A, Wolfrum C, Rudin M. Hepatic lipid composition differs between ob / ob and ob / + control mice as determined by using in vivo localized proton magnetic resonance spectroscopy. 2012;

46. Hamilton G, Yokoo T, Bydder M, Cruite I, Schroeder ME, Sirlin CB, et al. In vivo characterization of the liver fat 1H MR spectrum. NMR Biomed. 2011;24(7):16.

47. Kraemer FB. Hormone-sensitive lipase: control of intracellular tri-(di-)acylglycerol and cholesteryl ester hydrolysis. J Lipid Res. 2002 Oct 1;43(10):1585–94.

48. Mead JR, Irvine SA, Ramji DP. Lipoprotein lipase: structure, function, regulation, and role in disease. J Mol Med (Berl). 2002 Dec;80(12):753–69.

49. Weijers RNM. Lipid composition of cell membranes and its relevance in type 2 diabetes mellitus. Curr Diabetes Rev. 2012 Sep;8(5):390–400.

50. Chow JDY, Lawrence RT, Healy ME, Dominy JE, Liao JA, Breen DS, et al. Genetic inhibition of hepatic acetyl-CoA carboxylase activity increases liver fat and alters global protein acetylation. Mol Metab. 2014 Jul;3(4):419–31.

51. Bozzetto L, Prinster A, Annuzzi G, Costagliola L, Mangione A, Vitelli A, et al. Liver fat is reduced by an isoenergetic MUFA diet in a controlled randomized study in type 2 diabetic patients. Diabetes Care. 2012 Jul 1;35(7):1429–35.

52. Anderson N, Borlak J. Molecular mechanisms and therapeutic targets in steatosis and steatohepatitis. Pharmacol Rev. 2008 Sep 1;60(3):311–57.

53. Puri P, Wiest MM, Cheung O, Mirshahi F, Sargeant C, Min H-K, et al. The plasma lipidomic signature of nonalcoholic steatohepatitis. Hepatology. 2009 Dec;50(6):1827–38.

54. Simões C, Domingues P, Ferreira R, Amado F, Duarte JA, Vitorino R, et al. Remodeling of liver phospholipidomic profile in streptozotocin-induced diabetic rats. Arch Biochem Biophys. 2013 Oct 15;538(2):95–102.

55. Ling PR, Boyce P, Bistrian BR. Role of arachidonic acid in the regulation of the inflammatory response in TNF-alpha-treated rats. JPEN J Parenter Enteral Nutr. Jan;22(5):268–75.

56. Elizondo A, Araya J, Rodrigo R, Poniachik J, Csendes A, Maluenda F, et al. Polyunsaturated fatty acid pattern in liver and erythrocyte phospholipids from obese patients. Obesity (Silver Spring). 2007 Jan;15(1):24–31.

57. Donovan EL, Pettine SM, Hickey MS, Hamilton KL, Miller BF. Lipidomic analysis of human plasma reveals ether-linked lipids that are elevated in morbidly obese humans compared to lean. Diabetol Metab Syndr. 2013 Jan;5(1):24.

58. Hanamatsu H, Ohnishi S, Sakai S, Yuyama K, Mitsutake S, Takeda H, et al. Altered levels of serum sphingomyelin and ceramide containing distinct acyl chains in young obese adults. Nutr Diabetes. Macmillan Publishers Limited; 2014 Jan 20;4:e141.

59. Paradies G, Paradies V, Ruggiero FM, Petrosillo G. Oxidative stress, cardiolipin and mitochondrial dysfunction in nonalcoholic fatty liver disease. World J Gastroenterol. 2014 Oct 21;20(39):14205–18.

60. Li Z, Agellon LB, Allen TM, Umeda M, Jewell L, Mason A, et al. The ratio of phosphatidylcholine to phosphatidylethanolamine influences membrane integrity and steatohepatitis. Cell Metab. 2006 May;3(5):321–31.

61. Cabrero C, Merida I, Ortiz P, Varela I, Mato JM. Effects of alloxan on S-adenosylmethionine metabolism in the rat liver. Biochem Pharmacol. 1986 Jul 1;35(13):2261–4.

62. Hoffman DR, Haning JA, Cornatzer WE. Effect of Alloxan Diabetes on Phosphatidylcholine Biosynthetic Enzymes. Exp Biol Med. SAGE Publications; 1981 Jun 1;167(2):143–6.

63. Chitraju C, Trötzmüller M, Hartler J, Wolinski H, Thallinger GG, Lass A, et al. Lipidomic analysis of lipid droplets from murine hepatocytes reveals distinct signatures for nutritional stress. J Lipid Res. 2012 Oct;53(10):2141–52.

64. Geelen MJ, Groener JE, De Haas CG, Van Golde LM. Influence of glucagon on the synthesis of phosphatidylcholines and phosphatidylethanolamines in monolayer cultures of rat hepatocytes. FEBS Lett. 1979 Sep 1;105(1):27–30.

65. Geelen MJ, Groener JE, de Haas CG, Wisserhof TA, van Golde LM. Influence of insulin and glucagon on the synthesis of glycerolipids in rat hepatocytes. FEBS Lett. 1978 Jun 1;90(1):57–60.

66. Quehenberger O, Armando AM, Brown AH, Milne SB, Myers DS, Merrill AH, et al. Lipidomics reveals a remarkable diversity of lipids in human plasma. J Lipid Res. 2010 Nov;51(11):3299–305.

67. Perry RJ, Camporez J-PG, Kursawe R, Titchenell PM, Zhang D, Perry CJ, et al. Hepatic Acetyl CoA Links Adipose Tissue Inflammation to Hepatic Insulin Resistance and Type 2 Diabetes. Cell. Elsevier; 2015 Feb 12;160(4):745–58.

68. Okamoto Y. Enhanced GLUT2 gene expression in an oleic acid-induced in vitro fatty liver model. Hepatol Res. 2002 Jun;23(2):138–44.

69. Santos JC de F, Valentim IB, de Araújo ORP, Ataide T da R, Goulart MOF. Development of nonalcoholic hepatopathy: contributions of oxidative stress and advanced glycation end products. Int J Mol Sci. 2013 Jan;14(10):19846–66.

70. He Y, Zhu J, Huang Y, Gao H, Zhao Y. Advanced glycation end product (AGE)-induced hepatic stellate cell activation via autophagy contributes to hepatitis C-related fibrosis. Acta Diabetol. 2015 May 24;

71. Yamagishi S, Matsui T. Role of receptor for advanced glycation end products (RAGE) in liver disease. Eur J Med Res. 2015 Jan;20:15.

72. Sharma M, Mitnala S, Vishnubhotla RK, Mukherjee R, Reddy DN, Rao PN. The Riddle of Nonalcoholic Fatty Liver Disease: Progression From Nonalcoholic Fatty Liver to Nonalcoholic Steatohepatitis. J Clin Exp Hepatol. Elsevier Ltd; 2015;5(2):147–58.

73. Patel R, Baker SS, Liu W, Desai S, Alkhouri R, Kozielski R, et al. Effect of dietary advanced glycation end products on mouse liver. PLoS One. 2012;7(4).

74. Yilmaz Y, Ulukaya E, Gul OO, Arabul M, Gul CB, Atug O, et al. Decreased plasma levels of soluble receptor for advanced glycation endproducts (sRAGE) in patients with nonalcoholic fatty liver disease. Clin Biochem. 2009 Jun;42(9):802–7.

75. Takeuchi M, Sakasai-Sakai A, Takata T, Ueda T, Takino J, Tsutsumi M, et al. Serum levels of toxic AGEs (TAGE) may be a promising novel biomarker in development and progression of NASH. Med Hypotheses. 2015 May;84(5):490–3.

76. Duarte N, Coelho IC, Patarrão RS, Almeida JI, Penha-Gonçalves C, Macedo MP. How Inflammation Impinges on NAFLD: A Role for Kupffer Cells. Biomed Res Int. 2015 Jan;2015:984578.